Molecular basis of synaptic vesicle cargo recognition by the endocytic sorting adaptor stonin 2

Nadja Jung,[1] Martin Wienisch,[2] Mingyu Gu,[3] James B. Rand,[4] Sebastian L. Müller,[5] Gerd Krause,[5] Erik M. Jorgensen,[3] Jürgen Klingauf,[2] and Volker Haucke[1]

[1]Department of Membrane Biochemistry, Institute of Chemistry and Biochemistry, Freie Universität Berlin, 14195 Berlin, Germany
[2]Department of Membrane Biophysics, Max-Planck-Institute for Biophysical Chemistry, 37077 Göttingen, Germany
[3]Department of Biology, University of Utah, Salt Lake City, UT 84112
[4]Program in Molecular, Cell and Developmental Biology, Oklahoma Medical Research Foundation, Oklahoma City, OK 73104
[5]Leibniz-Institut für Molekulare Pharmakologie, 13125 Berlin, Germany

Synaptic transmission depends on clathrin-mediated recycling of synaptic vesicles (SVs). How select SV proteins are targeted for internalization has remained elusive. Stonins are evolutionarily conserved adaptors dedicated to endocytic sorting of the SV protein synaptotagmin. Our data identify the molecular determinants for recognition of synaptotagmin by stonin 2 or its *Caenorhabditis elegans* orthologue UNC-41B. The interaction involves the direct association of clusters of basic residues on the surface of the cytoplasmic domain of synaptotagmin 1 and a β strand within the μ–homology domain of stonin 2. Mutation of K783, Y784, and E785 to alanine within this stonin 2 β strand results in failure of the mutant stonin protein to associate with synaptotagmin, to accumulate at synapses, and to facilitate synaptotagmin internalization. Synaptotagmin-binding–defective UNC-41B is unable to rescue paralysis in *C. elegans* stonin mutant animals, suggesting that the mechanism of stonin-mediated SV cargo recognition is conserved from worms to mammals.

Introduction

Efficient synaptic vesicle (SV) endocytosis is essential to maintain the ability of the synapse to release neurotransmitter under sustained stimulation. Strong evidence suggests that the clathrin-based endocytic machinery is required to recognize and properly sort SV proteins during the generation of functional SVs (Brodin et al., 2000; Murthy and De Camilli, 2003; Galli and Haucke, 2004; Sudhof, 2004), even at small central synapses (Granseth et al., 2006). In spite of this, the precise molecular mechanism of SV cargo recognition has remained elusive. Although conventional endocytic sorting signals, such as tyrosine- or dileucine-based motifs (Bonifacino and Traub, 2003), may target cargo proteins for constitutive internalization by the heterotetrameric adaptor assembly protein complex 2 (AP-2; comprising α, β2, μ2, and σ2 subunits), no common endocytic sorting signals have been identified for SV proteins. One possibility is that SV proteins remain preassembled (Bennett et al., 1992; Willig et al., 2006), possibly by cholesterol-rich microdomains (Jia et al., 2006). Alternatively, SV proteins may undergo rapid postfusion reclustering to allow efficient recapturing by the endocytic machinery. Both of these scenarios would alleviate the need for an endocytic sorting signal within each individual SV protein. Instead, SV recycling may depend on the specific recognition of one (Voglmaier et al., 2006) or a few SV proteins by endocytic adaptors.

A likely candidate to connect the exo- and endocytic limbs of the SV cycle is synaptotagmin 1. Genetic, antibody-mediated, or chemical perturbation of synaptotagmin 1 function leads to partial vesicle depletion and SV recycling defects in the squid giant synapse (Llinas et al., 2004), at the *Drosophila melanogaster* neuromuscular junction (DiAntonio et al., 1993; Poskanzer et al., 2003), in *Caenorhabditis elegans* (Jorgensen et al., 1995), and in mammalian central nervous system synapses (Nicholson-Tomishima and Ryan, 2004). Synaptotagmin 1 also appears to influence the recycling efficiency of other SV proteins (Poskanzer et al., 2003; Nicholson-Tomishima and Ryan, 2004) through specific regions in its cytoplasmic tail (Poskanzer et al., 2006). The molecular mechanism underlying the function of synaptotagmin in SV endocytosis has remained uncertain but may involve its ability to associate with phosphoinositides (Bai et al., 2004), AP-2μ (Zhang et al., 1994; Chapman

Correspondence to Volker Haucke: v.haucke@biochemie.fu-berlin.de

Abbreviations used in this paper: AP-2, assembly protein complex 2; CLASP, clathrin-associated sorting protein; HEK, human embryonic kidney; μHD, μ–homology domain; NIE, neuroimmune endocrine; SV, synaptic vesicle; WT, wild type.

The online version of this paper contains supplemental material.

The Journal of Cell Biology, Vol. 179, No. 7, December 31, 2007 1497–1510
http://www.jcb.org/cgi/doi/10.1083/jcb.200708107

Supplemental Material can be found at:
http://www.jcb.org/cgi/content/full/jcb.200708107/DC1

et al., 1998; Grass et al., 2004), or the endocytic adaptor stonin 2 (termed stoned B in flies and UNC-41 in *C. elegans*; Fergestad and Broadie, 2001; Martina et al., 2001; Stimson et al., 2001; Walther et al., 2004).

Stonin 2 represents the first, and so far only, endocytic protein specifically dedicated to SV recycling by acting as a sorting adaptor for synaptotagmin 1 (Diril et al., 2006). Expression of stonin 2 in fibroblasts is sufficient to rescue clathrin/AP-2–mediated internalization of surface-stranded synaptotagmin 1 (Jarousse and Kelly, 2001) and facilitates synaptotagmin 1 redistribution into SVs in primary neurons (Diril et al., 2006). Stonin 2 is linked to the endocytic machinery by direct interactions with AP-2 (Walther et al., 2004) and eps15 or intersectin (Martina et al., 2001), and can therefore be classified as a clathrin-associated sorting protein (CLASP; Traub, 2005). CLASPs compose a set of adaptors, including β-arrestins (Lefkowitz and Whalen, 2004), autosomal recessive hypercholesterolemia (Edeling et al., 2006), Dab2 (Mishra et al., 2002), Huntingtin interacting protein 1/1R, and numb (Santolini et al., 2000), that target specific cargo to clathrin-coated pits or subsets thereof for regulated internalization.

In contrast to other CLASPs, we lack detailed molecular information on how stonin 2 and its orthologues recognize SV cargo during exo- and endocytic vesicle cycling. We demonstrate that an evolutionarily conserved β strand within the μ–homology domain (μHD) of stonin 2 recognizes basic patches on the surface of the cytoplasmic domain of synaptotagmin 1. Mutation of critical residues within this β strand results in failure of the mutant stonin protein to physically associate with synaptotagmin and to facilitate synaptotagmin internalization in fibroblasts or primary neurons. Furthermore, synaptotagmin-binding–defective UNC-41B is unable to rescue paralysis in *C. elegans unc-41*/stonin mutant animals, suggesting that the mechanism of stonin-mediated SV cargo recognition is conserved from worms to mammals.

Results

Stonin 2 physically and functionally interacts with the C2A domain of synaptotagmin 1 to facilitate internalization

Given the importance of functional SV recycling and the role of synaptotagmin 1 in coupling exo- and endocytosis in neuro secretory cells, we first set out to identify the domains required for its internalization. Expression of stonin 2 in human embryonic kidney (HEK) 293 cells stably transfected with FLAG–synaptotagmin 1 leads to redistribution of synaptotagmin 1 from the plasma membrane to internal compartments (Diril et al., 2006). Internalization assays based on anti-FLAG antibody uptake showed that endocytosed synaptotagmin localizes to a subset of AP-2–coated puncta and to a perinuclear endosomal compartment (Fig. 1 A; Diril et al., 2006), suggesting that stonin 2 targets synaptotagmin 1 to clathrin/AP-2–coated pits. To confine the region within synaptotagmin 1 required for stonin 2–mediated internalization deletion, constructs lacking one or both of the C2 domains were generated and analyzed by antibody uptake experiments. After antibody chase for 20 min at 37°C, surface-stranded synaptotagmin 1 was detected by Alexa Fluor 594–labeled secondary antibodies under non-permeabilizing conditions, remaining surface immunoreactivity was blocked, and internalized synaptotagmin 1 was revealed using Alexa Fluor 488–labeled secondary antibodies. Surprisingly, we found that synaptotagmin 1 lacking the C2B domain (syt1ΔC2B) was internalized, albeit with reduced efficiency, whereas mutant proteins lacking either the C2A (syt1ΔC2A) or both C2 domains (syt1ΔC2AB) were not endocytosed (Fig. 1 B). Thus, the C2A domain contributes the major internalization signal for stonin 2–dependent synaptotagmin 1 endocytosis. This interpretation is supported by membrane recruitment experiments in N1E neuroblastoma cells. Overexpression of wild-type (WT) synaptotagmin 1 or syt1ΔC2B, but not syt1ΔC2A, caused a redistribution of WT stonin 2 (stonin 2^{WT}; Diril et al., 2006) or an AP-2 and Eps15 homology domain–binding–defective stonin 2 mutant (stonin $2^{\delta WF\delta NPF}$, used to exclude indirect effects mediated via AP-2 or, e.g., eps15) from the cytosol to the plasmalemma (Fig. 1 C). Stonin 2 coimmunoprecipitated with WT synaptotagmin 1 or syt1ΔC2B but not with syt1ΔC2A, which is consistent with the microscopic data (Fig. 1 D). AP-2 was found in the same complex, presumably because of its direct interaction with stonin 2. This complex was also seen in affinity chromatography experiments using extracts from transfected HEK cells incubated with GST-fused C2 domains (Figs. S1 A and S2 B, available at http://www.jcb.org/cgi/content/full/jcb.200708107/DC1). Stonin 2^{WT} or stonin $2^{\delta WF\delta NPF}$ preferentially associated with the C2A domain of synaptotagmin 1. AP-2 efficiently copurified with either C2A or C2B from cell extracts containing stonin 2^{WT} but was predominantly retained by C2B if lysates from stonin $2^{\delta WF\delta NPF}$–expressing cells were used (Fig. S1, A and B), which is in agreement with published data (Chapman et al., 1998; Haucke et al., 2000). To further corroborate the direct association of stonin 2 with synaptotagmin 1–C2A, we performed in vitro binding experiments using GST-fused synaptotagmin 1 and His_6-tagged stonin 2 purified from HEK293 fibroblasts (Fig. S2 B). Stonin 2 most efficiently bound to GST-C2A or -C2AB, whereas a much weaker interaction with the C2B domain was observed (Fig. 2 A). Stonin 2 did not bind to GST control beads. These results were confirmed by experiments using ^{35}S-labeled stonin 2 synthesized by coupled transcription/translation in vitro (Fig. S2 A). We conclude that stonin 2 directly associates with synaptotagmin 1, mainly via determinants in the C2A domain.

Stonin 2 recognizes basic patches within the synaptotagmin 1 C2 domains

Coimmunoprecipitation experiments from transfected fibroblasts (Fig. S3, available at http://www.jcb.org/cgi/content/full/jcb.200708107/DC1) indicated that the major binding site for synaptotagmin 1 comprised the carboxy-terminal μHD of stonin 2. The μHD exhibits ∼30% amino acid identity with the μ2 subunit of AP-2, which associates with a stretch of basic amino acid residues within the C2B domain of synaptotagmin 1 (Chapman et al., 1998; Grass et al., 2004). Considering the homology between AP-2μ and the stonin 2 μHD and the existence of basic patches in both C2 domains, we rationalized that basic residues might play a role in stonin 2 binding. To test this,

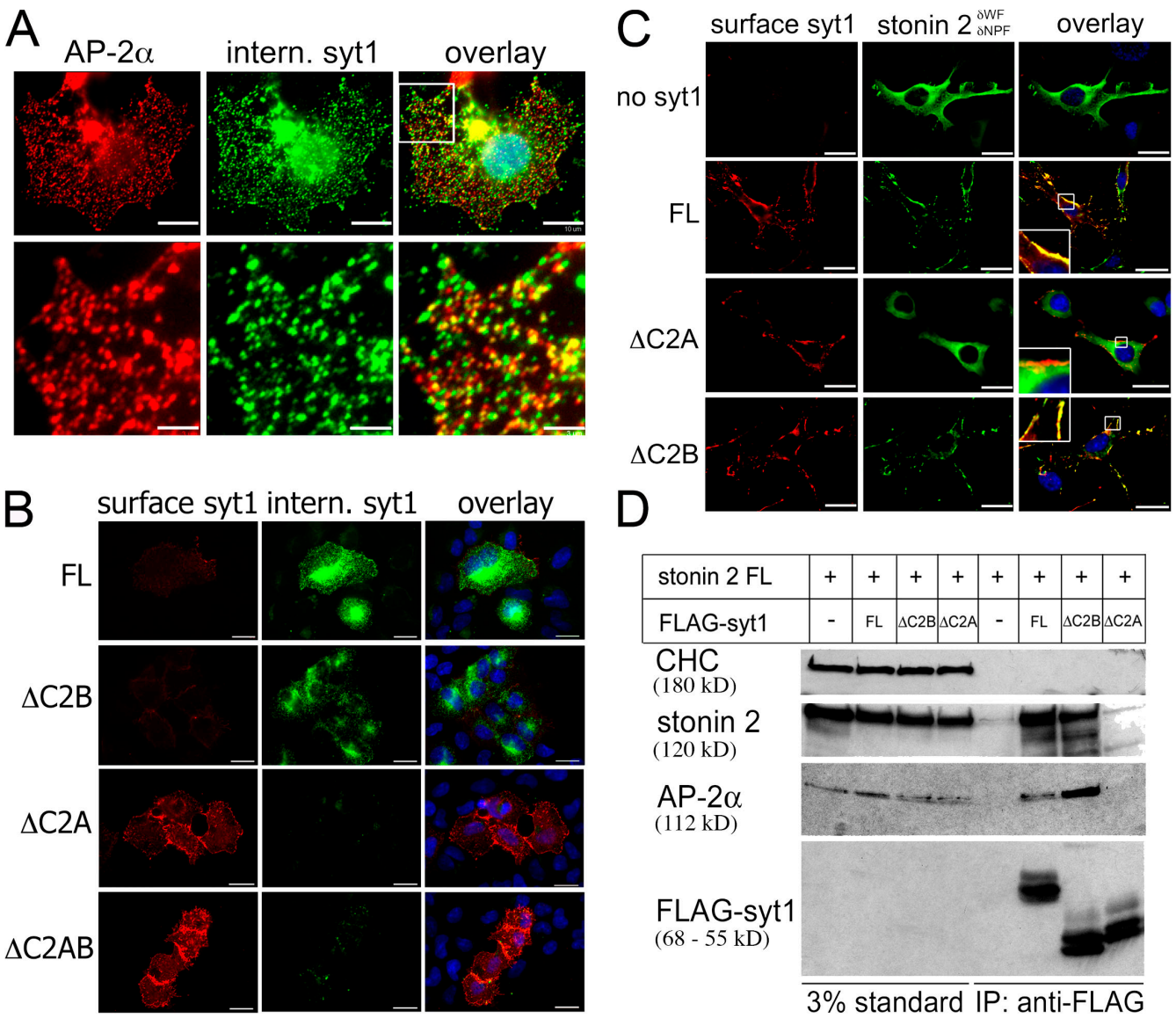

Figure 1. **The synaptotagmin 1 C2A domain is required for stonin 2–mediated synaptotagmin 1 internalization.** (A) Stonin 2 recruits synaptotagmin 1 to AP-2–coated puncta. HEK293 cells stably expressing FLAG–synaptotagmin 1 were subjected to anti-FLAG antibody uptake experiments. Internalized synaptotagmin 1 (green) colocalizes partially with endogenous AP-2 (red) in plasmalemmal puncta (yellow), presumably representing clathrin/AP-2–coated pits. Blue, DAPI-stained nuclei. Images were obtained by deconvolution fluorescence microscopy. White boxes indicate magnified areas below. Bars: (top) 10 μm; (bottom) 3 μm. (B) HEK293 cells coexpressing HA-tagged stonin 2 and FLAG–synaptotagmin 1 C2 domain deletion mutants were analyzed by antibody uptake assays as described in A. Surface-exposed (red) or internalized (green) synaptotagmin 1 was labeled with Alexa Fluor594– or 488–conjugated secondary antibodies, respectively. Blue, DAPI-stained nuclei. Equal exposure times and identical intensity normalization were used during the acquisition of the images. Bars, 20 μm. (C) The C2A domain is required for membrane recruitment of stonin 2. NIE cells were cotransfected with AP-2–binding–deficient HA-stonin $2^{\delta WF\delta NPF}$ and FLAG–synaptotagmin 1 deletion constructs. The distribution of surface synaptotagmin 1 (red) and stonin 2 (green) were analyzed by deconvolution fluorescence microscopy. Blue, DAPI-stained nuclei. White boxes indicate magnified areas to the right. Bars, 20 μm. (D) Deletion of the C2A domain results in loss of stonin 2 binding in coimmunoprecipitation experiments. HEK293 cells were cotransfected with HA-tagged stonin 2 and FLAG-tagged synaptotagmin 1 deletion constructs. Immunoprecipitation was performed using antibodies directed against the FLAG tag. Immunoprecipitated proteins were detected by immunoblotting for clathrin heavy chain (CHC) as control, HA-tag (stonin 2), α-adaptin (AP-2α), and FLAG-tag (syt1). 3% of the input material was loaded as standard.

we generated synaptotagmin 1 mutants by exchanging K or R residues within basic patches of C2A or C2B for alanines (Fig. 2 B). Additionally, we targeted for mutation residues within C2A that were not conserved between synaptotagmins 1 and 6 (Fig. 2B, C2A mut 4). Synaptotagmin 6 is an isoform that appears to lack the ability to interact with stonin 2 in living cells (Diril et al., 2006). C2A and C2B mutants were then tested for their ability to associate with AP-2 or stonin $2^{\delta WF\delta NPF}$ in pull-down experiments from transfected fibroblasts. We found that the elimination of basic residues within either C2 domain severely reduced binding to AP-2 or stonin $2^{\delta WF\delta NPF}$. Exchange of six basic residues within C2B attenuated association with stonin 2 or AP-2 binding below detection limits (Fig. S1 C). AP-2 binding to the C2A domain was abolished by elimination of two or more basic residues within C2A. We still observed some residual binding of stonin 2 to a C2A mutant in which six basic

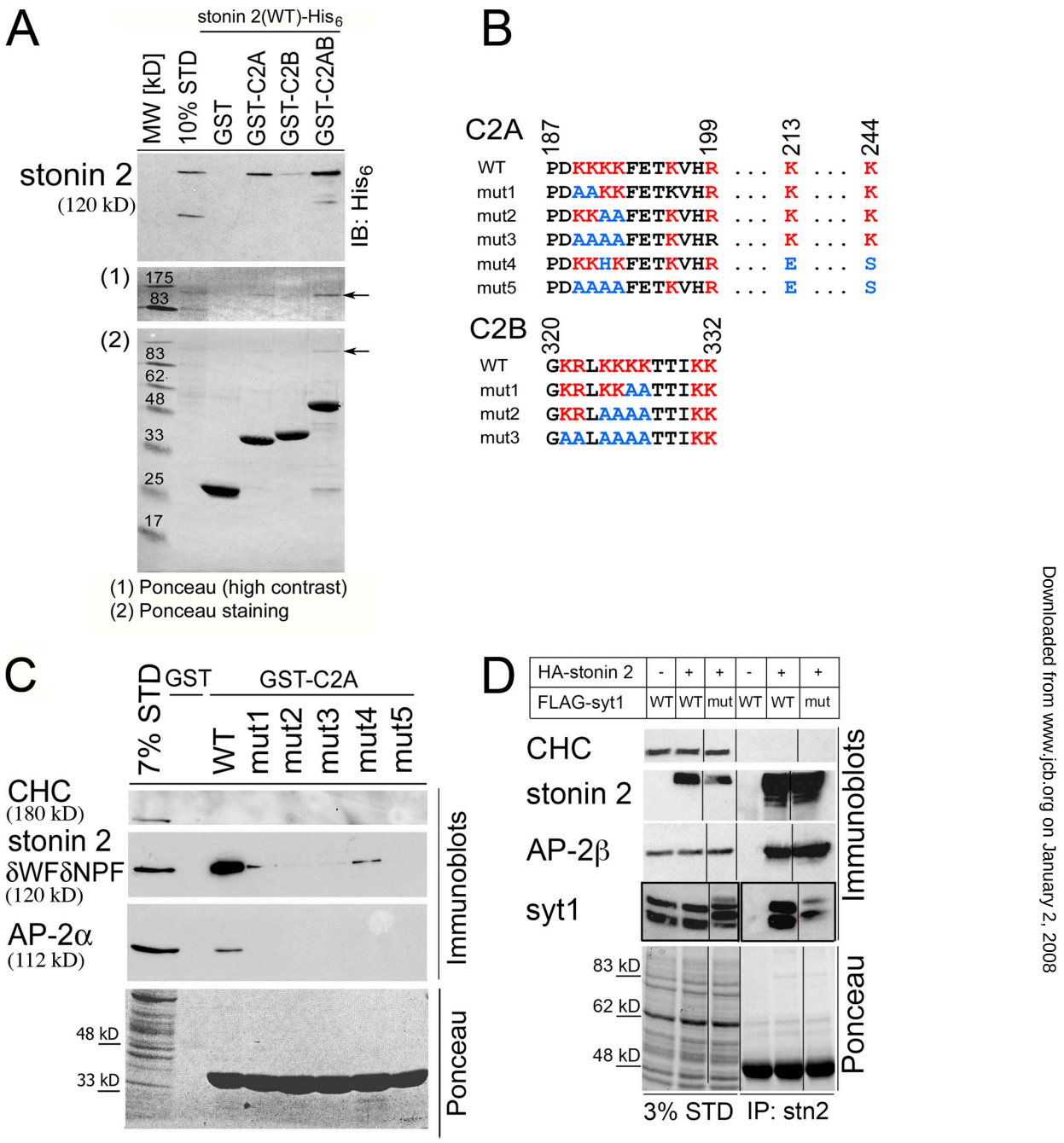

Figure 2. **Clusters of basic amino acids within the synaptotagmin 1 C2 domains are involved in the association with stonin 2.** (A) Stonin 2 and synaptotagmin 1–C2A interact directly. Stonin 2–His_6 was purified from stably transfected HEK293 cells and incubated with GST–synaptotagmin 1 fusion proteins immobilized on beads. Bound stonin 2 was detected by immunoblotting for the His_6-tag. Arrows mark bound stonin 2 on the Ponceau-stained nitrocellulose membrane. 10% of the input was loaded as standard (STD). Molecular masses are indicated. (B) Alignment of basic patches within synaptotagmin 1 C2A and C2B domains and mutants analyzed. (C) GST-C2A WT or mutant fusion proteins (see B) were assayed in pulldown experiments for their ability to associate with HA–stonin $2^{\delta WF\delta NPF}$ from HEK293 lysates. Samples were analyzed by immunoblotting for HA–stonin 2, AP-2β, and clathrin heavy chain (CHC). 7% of the input was loaded as standard. (D) Coimmunoprecipitation experiment performed from cotransfected fibroblasts. HEK293 cells were cotransfected with HA-tagged stonin 2 and FLAG-tagged synaptotagmin 1 WT and mutant (K189–191E; K213E; K244E; KR321, 322EE; and K324–327EE) constructs. Immunoprecipitation was performed using polyclonal antiserum against stonin 2. Immunoblotting was performed using antibodies against HA-stonin 2, AP-2β, anti–FLAG–synaptotagmin 1, and anti–clathrin heavy chain antibodies. 3% of the input was loaded as standard. Splices are indicated by solid lines (all taken from the same exposure). In the case of FLAG–synaptotagmin 1, the bands representing material present in 3% of the starting material were taken from a slightly longer exposure of the x-ray film from the same immunoblot to reveal the bands. The two exposures are indicated by black boxes. Black lines indicate that intervening lanes have been spliced out.

residues had been exchanged (Fig. 2 C). These data were confirmed by coimmunoprecipitation experiments using charge reversal mutants of synaptotagmin 1. A synaptotagmin 1 mutant in which six basic side chains had been exchanged for acidic ones (K189–191E, K213E, K244E; KR321, K322EE; and K324–327E) displayed strongly reduced binding to stonin 2,

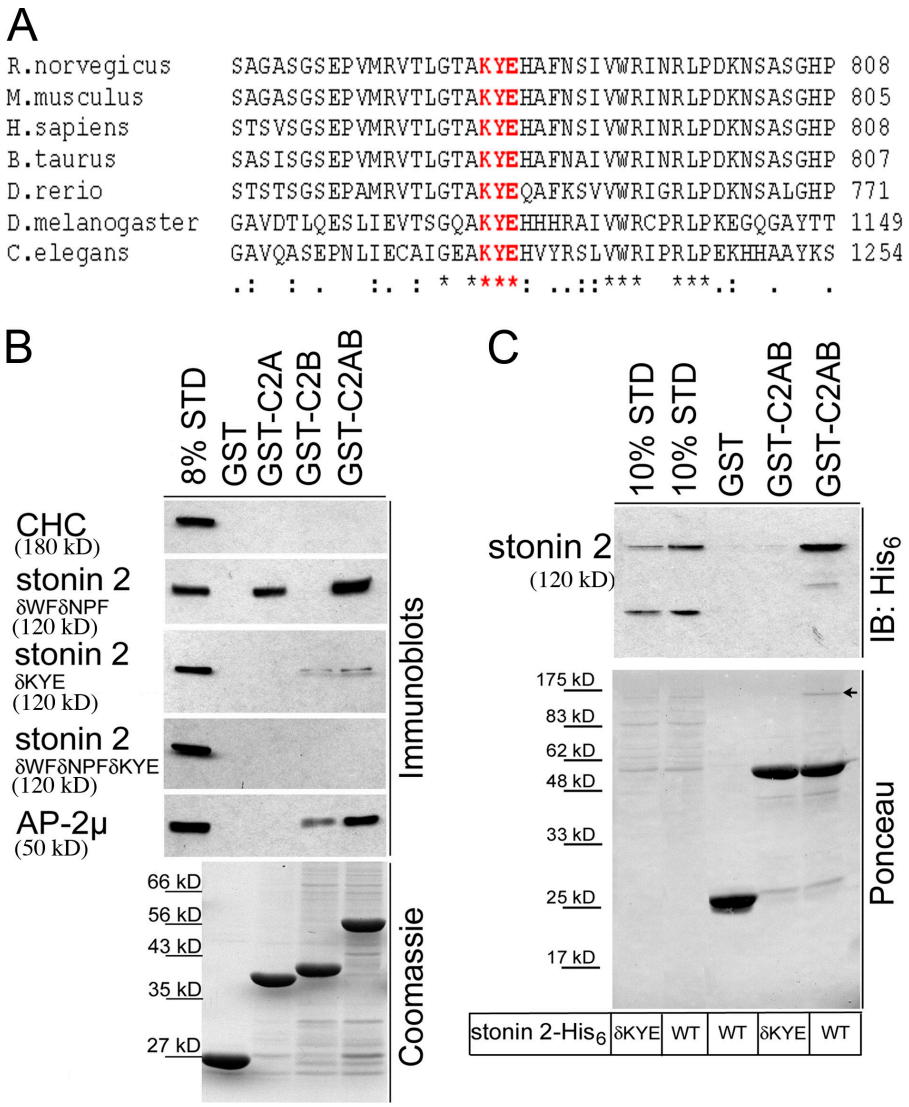

Figure 3. **Evolutionarily conserved residues within a β strand of its μHD are required for association of stonin 2 with synaptotagmin 1.** (A) The KYE site is evolutionarily conserved. Multiple protein sequence alignment of stonin 2 and orthologues from rat, mouse, human, cattle, zebrafish, *D. melanogaster*, and *C. elegans*. Numbers refer to the last amino acid residue within the predicted β strand. Conserved residues K783, Y784, and E785 are colored in red. (B) Mutation of conserved residues K783A, Y784A, and E785A within stonin 2 abolishes its ability to bind to synaptotagmin 1. GST–synaptotagmin 1 fusion proteins immobilized on beads were incubated with cell extracts derived from HEK293 cells transfected with AP-2–binding–deficient HA–stonin $2^{\delta WF\delta NPF}$, HA–stonin $2^{\delta KYE}$, or HA–stonin $2^{\delta WF\delta NPF\delta KYE}$, respectively. Bound proteins were detected by immunoblotting for clathrin heavy chain (CHC), HA–stonin 2, and AP-2μ. 8% of the input was loaded as standard (STD). (C) In vitro binding experiment using purified recombinant proteins. GST-C2AB immobilized on beads was incubated with purified stonin 2–His_6 WT or δKYE. Bound stonin 2–His_6 was detected by immunoblotting for the His_6-tag. The arrow marks the stonin 2–His_6 band on the Ponceau S–stained nitrocellulose membrane. 10% of the input was loaded as standard.

although the interaction was not abolished completely (Fig. 2 D), indicating that additional, perhaps cooperative, mechanisms might be at work. In summary, we identify basic patches within both C2 domains of synaptotagmin 1 as the major determinants for association with stonin 2.

The KYE site within the stonin 2 μHD is required for synaptotagmin 1 interaction and internalization

We observed that stonin 2 associated via its μHD (Fig. S3, A and B) with basic residues within the synaptotagmin 1 C2 domains, which is similar to the interaction between AP-2μ and synaptotagmin 1 C2B. Hence, we hypothesized that these interactions might be structurally related. Previous studies had suggested that a β strand comprising residue Y343 within subdomain B of AP-2μ is part of the synaptotagmin 1 binding site (Haucke et al., 2000). Structural data are available for AP-2 (Owen and Evans, 1998; Collins et al., 2002) including its μ2 subunit, which displays high sequence homology (~52%) to the carboxy-terminal region of stonin 2. We used μ2 as a template to generate a molecular homology model of the stonin 2 μHD (Fig. S3 D). The stonin 2 μHD model displays an overall β-fold structure very similar to that of AP-2μ, except for a few loops that differ from the template. Conserved features include the β strand suggested to harbor the synaptotagmin binding site within AP-2μ, which contains the aforementioned tyrosine residue (Y343 in AP-2μ). This tyrosine (corresponding to Y784 in human stonin 2), as well as several flanking residues, is also evolutionarily conserved within stonin family members from humans to nematodes (Fig. 3 A), which is suggestive of its functional importance.

We hypothesized that Y784 and its neighbors form part of the binding site for synaptotagmin 1. To test this, we generated a stonin 2 mutant in which residues K783, Y784, and E785 (Fig. 3 A, red; and Fig. S3 D, right, red) had been exchanged by alanines (stonin $2^{\delta KYE}$). We transfected fibroblasts with stonin $2^{\delta WF\delta NPF}$, the KYE mutant stonin 2 (stonin $2^{\delta KYE}$), or a mutant of stonin 2 combining these mutations (stonin $2^{\delta WF\delta NPF\delta KYE}$) and performed affinity chromatography experiments using immobilized GST-fused synaptotagmin 1 C2 domains. Although stonin $2^{\delta WF\delta NPF}$ readily copurified with synaptotagmin 1 C2A or AB, the double mutant of stonin 2 (stonin $2^{\delta WF\delta NPF\delta KYE}$) had completely

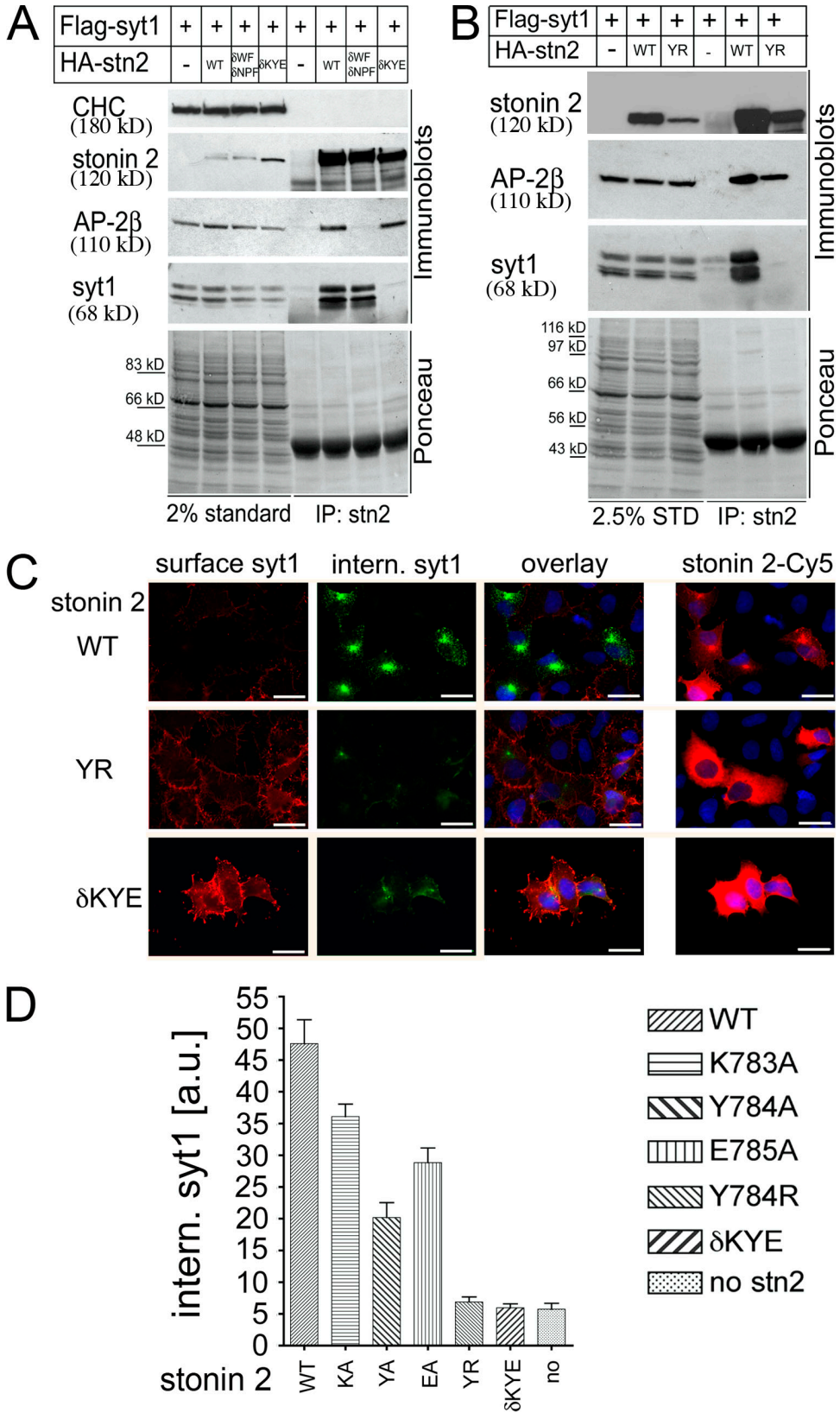

Figure 4. **Stonin 2–mediated synaptotagmin 1 internalization requires an intact KYE site within stonin 2.** (A) Synaptotagmin 1 does not associate with mutant stonin $2^{\delta KYE}$ in coimmunoprecipitation experiments. HEK293 cells were cotransfected with FLAG–synaptotagmin 1 and HA–stonin 2^{WT}, AP-2–binding–deficient HA–stonin $2^{\delta WF\delta NPF}$, or HA–stonin $2^{\delta KYE}$, respectively. Proteins immunoprecipitated with antibodies against stonin 2 were detected by immunoblotting for HA–stonin 2, AP-2β, FLAG–synaptotagmin 1, and clathrin heavy chain (CHC). 2% of the input was loaded as standard. (B) The Y784R point mutant of stonin 2 is unable to associate with synaptotagmin 1. Experiments were done as described in A. 2.5% of the input was loaded as standard. (C) Stonin $2^{\delta KYE}$ and stonin 2^{YR} mutants lack the ability to facilitate synaptotagmin 1 internalization. HEK-syt1 cells were transfected with HA-tagged stonin 2^{WT}, stonin $2^{\delta KYE}$, or

lost its ability to associate with synaptotagmin (Fig. 3 B). Trace amounts of stonin $2^{\delta KYE}$ were retained on GST-C2B– or -C2AB–containing beads. This is owed to the fact that this mutant retains the ability to bind to AP-2 (Fig. 4 A) and, thus, indirectly associates with the C2B domain of synaptotagmin 1 via AP-2. Similar results were obtained in direct binding experiments using His_6-tagged stonin $2^{\delta KYE}$ purified from HEK cells (Fig. 3 C) or synthesized by coupled transcription/translation in vitro (Fig. S3 C).

To further corroborate these findings, we performed coimmunoprecipitation experiments. Fibroblasts were cotransfected with synaptotagmin 1 and stonin 2^{WT}, stonin $2^{\delta WF\delta NPF}$, or the δKYE mutant of stonin 2. As expected, synaptotagmin 1 was found in immunoprecipitates containing stonin 2^{WT} or stonin $2^{\delta WF\delta NPF}$ but not stonin $2^{\delta KYE}$. Conversely, stonin $2^{\delta KYE}$, but not stonin $2^{\delta WF\delta NPF}$, retained its ability to associate with AP-2 (Fig. 4 A). Similar results were seen for a stonin 2 mutant in which Y784 had been exchanged for R (stonin 2^{YR}; Fig. 4 B). This was corroborated in direct binding assays using ^{35}S-labeled stonin 2^{YR} (Fig. S3 C). To exclude the possibility that the introduced mutations negatively impact protein folding and, therefore, nonspecifically affect synaptotagmin binding, we probed the structure of the generated stonin 2 mutants by limited proteolysis. The digestion patterns of stonin 2^{WT}, stonin $2^{\delta KYE}$, and stonin 2^{YR} were not found to be significantly different (Fig. S4, available at http://www.jcb.org/cgi/content/full/jcb.200708107/DC1), excluding gross structural changes induced by the mutations.

Synaptotagmin-binding–defective stonin 2 is unable to facilitate synaptotagmin 1 internalization in fibroblasts or neurons and fails to accumulate at synapses

To study the functional importance of the interaction between stonin 2 and synaptotagmin 1, we performed endocytosis experiments in HEK–synaptotagmin 1 cells coexpressing either stonin 2^{WT} or synaptotagmin 1–binding–deficient mutants thereof. Neither stonin $2^{\delta KYE}$ nor stonin 2^{YR} mutants were able to facilitate AP-2–dependent synaptotagmin 1 internalization (Fig. 4, C and D). Stonin $2^{\delta KYE}$ and stonin 2^{YR} also failed to become recruited to the plasmalemma by overexpressed synaptotagmin 1 in N1E neuroblastoma cells (Fig. 5). Quantitative fluorescence-based analysis of synaptotagmin 1 internalization indicated that mutations of individual residues within the KYE site to alanines reduced the efficiency of endocytosis and that these effects were additive (Fig. 4 D). Based on these findings, we conclude that the direct association between stonin 2 and synaptotagmin 1 is necessary for the physiological function of stonin 2 as a synaptotagmin-specific endocytic sorting adaptor.

In primary neurons, stonin 2 localizes to pre-SV clusters (Diril et al., 2006). We hypothesized that this localization might be caused by its interaction with synaptotagmin 1, at least in part. We transfected primary rat hippocampal neurons with HA-tagged stonin 2^{WT}, stonin $2^{\delta KYE}$, or stonin 2^{YR}, respectively, and studied their localization by indirect immunofluorescence microscopy. As expected, stonin 2^{WT} colocalized with synaptotagmin 1 in pre-SV clusters. In contrast, we were unable to detect such colocalization in the case of the synaptotagmin-binding–defective stonin 2 mutants, stonin $2^{\delta KYE}$, or stonin 2^{YR} (Fig. 6 A). Thus, stonin 2 represents the first example of an endocytic protein known to be targeted to synapses by interaction with a SV protein, further emphasizing its important role as a specialized adaptor dedicated to SV recycling.

We then quantitatively analyzed the effect of stonin 2^{WT} or the synaptotagmin-binding–defective KYE mutant on the partitioning of synaptotagmin 1 between the presynaptic plasmalemma or an internal SV-localized pool in primary hippocampal neurons in culture. To this aim, we used a previously described approach using ecliptic pHluorin-tagged synaptotagmin 1 (sytpHluorin). SytpHluorin is properly targeted to synapses where it undergoes activity-dependent exo-endocytic cycling (Diril et al., 2006). The pH dependence of the pHluorin fluorescence allows quantitative monitoring of the distribution of the synaptotagmin chimera (Wienisch and Klingauf, 2006). Fluorescence analysis after acid quenching and ammonium dequenching (Fig. 6, B and C) revealed that coexpression of stonin 2^{WT} significantly decreased the relative steady-state plasmalemmal fraction of sytpHluorin at presynaptic boutons, resulting in a strong increase of the vesicular/surface stranded pool ratio, as reported previously (Diril et al., 2006). In contrast, stonin $2^{\delta KYE}$ had lost the ability to facilitate targeting of sytpHluorin to the recycling vesicle pool but instead displayed a modest, albeit statistically insignificant, dominant-negative effect, i.e., led to a small decrease in the vesicular/surface stranded pool ratio of sytpHluorin (Fig. 6 D). Thus, the ability of stonin 2 to associate with synaptotagmin 1 is essential for its role as a synaptotagmin-specific sorting adaptor in neurons.

Synaptotagmin-binding–defective UNC-41B is unable to rescue paralysis in *C. elegans* mutant animals

As mentioned in the preceding paragraph, the μHD of stonins, and in particular the KYE site responsible for its association with synaptotagmin 1, is highly conserved between different stonin family members from mice to worms (Fig. 3 A). The *C. elegans* genome contains a single member of the stonin family encoded by *unc-41*, expressed as two alternative transcripts A and B (unpublished data). UNC-41B expressed in fibroblasts, like its mammalian counterpart stonin 2, was able to associate with the C2 domains of synaptotagmin 1, which is consistent with its putative role in SV recycling. Mutation of the KYE site within UNC-41B strongly impaired its synaptotagmin 1– binding ability (Fig. 7 A). To investigate whether UNC-41 plays a

stonin 2^{YR}, respectively. Synaptotagmin 1 internalization was assayed as described in the Fig. 1 legend. Red, surface synaptotagmin 1; green, internal synaptotagmin 1; blue, DAPI-stained nuclei. Stonin 2 expression was verified using Cy5-labeled secondary antibodies (right). Equal exposure times and identical intensity normalization were used during image acquisition. Bars, 20 μm. (D) Quantifications of synaptotagmin internalization experiments using stonin 2 mutants. Fluorescence intensities were quantified by applying the Mask function of the Slidebook 4.0.8 Digital Microscopy Software (Intelligent Imaging Innovations) on the green channel (internalized synaptotagmin 1) in stonin 2–transfected cells (red). Error bars represent SEM.

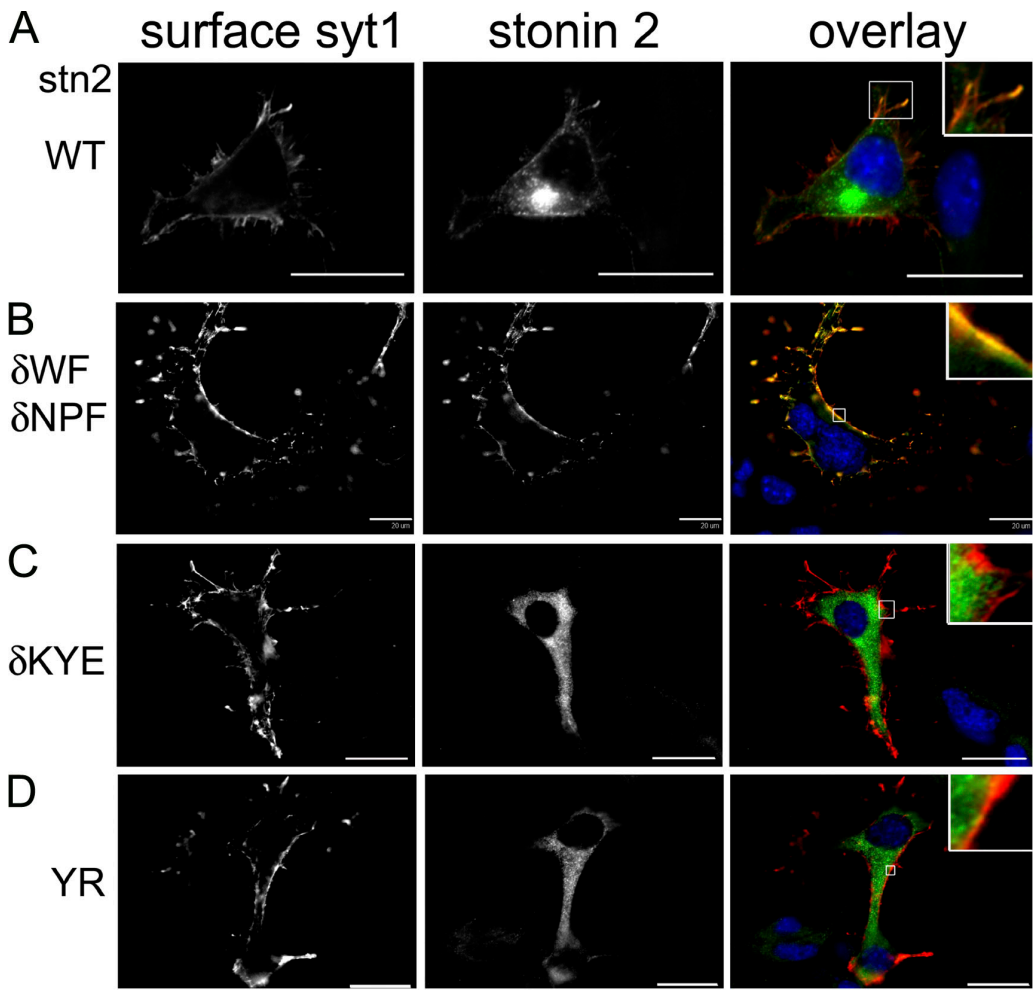

Figure 5. **The stonin 2 KYE site is required for synaptotagmin 1–dependent recruitment of stonin 2 to the plasmalemma in neuroblastoma cells.** NIE cells were cotransfected with lumenally FLAG-tagged synaptotagmin 1 and HA-tagged stonin 2^{WT} (A), AP-2–binding–deficient stonin $2^{\delta WF\delta NPF}$ (B), stonin $2^{\delta KYE}$ (C), or stonin 2^{YR} (D), respectively. Surface synaptotagmin 1 was labeled by anti-FLAG antibodies (red). After permeabilization, stonin 2 was immunostained using antibodies directed against stonin 2 (green). White boxes indicate magnifications to the right. Bars, 20 μm.

role in neurotransmission, we monitored animal movement. As expected, *unc-41(e268)* mutant worms carrying a nonsense mutation that abrogates UNC-41 protein expression displayed severe locomotion defects, presumably because of impaired neurotransmission. This phenotype was rescued by microinjection of a construct expressing WT UNC-41B cDNA but not the synaptotagmin interaction–defective δKYE mutant (Fig. 7, B and C), although both proteins were expressed at roughly similar levels (Fig. 7 D). Moreover, a 25-fold increase in injection concentration of the δKYE mutant protein-encoding plasmid also did not result in rescue of the locomotory phenotype (unpublished data). Similar results were seen in rescue experiments using GFP-tagged UNC-41B variants (unpublished data). When analyzed by confocal microscopy, WT GFP–UNC-41B exhibited a punctate synaptic distribution within the *C. elegans* nervous system, whereas the δKYE mutant protein failed to accumulate at synapses (Fig. 7 E). These experiments suggest that the KYE site is important for UNC-41B association with synaptotagmin and its targeting to synapses, although at this stage we cannot rule out the possibility that other factors contribute to this phenotype in vivo.

In summary, our data reveal the molecular basis for the recognition of synaptotagmin 1 by stonin 2 and suggest an evolutionarily conserved mechanism of cargo recognition by stonin family members during exo-endocytic SV cycling.

Discussion

This study provides the first detailed molecular characterization of the interaction interface between the SV protein–specific CLASP stonin 2 and its cargo, synaptotagmin 1. Previous studies have implicated the synaptotagmin 1 C2B domain in clathrin/AP-2–mediated endocytosis and SV recycling (Haucke et al., 2000; Littleton et al., 2001; Poskanzer et al., 2006). We demonstrate a role for the synaptotagmin 1 C2A domain as the main recognition site for stonin 2 and as a major determinant for synaptotagmin 1 internalization. The following lines of evidence support this. First, we find that synaptotagmin 1, lacking the C2B domain, is readily internalized in a stonin 2–dependent manner in transfected fibroblasts. Second, stonin 2 is recruited to the plasma membrane of transfected neuroimmune endocrine (NIE) cells by synaptotagmin 1 ΔC2B but not by a ΔC2A domain mutant.

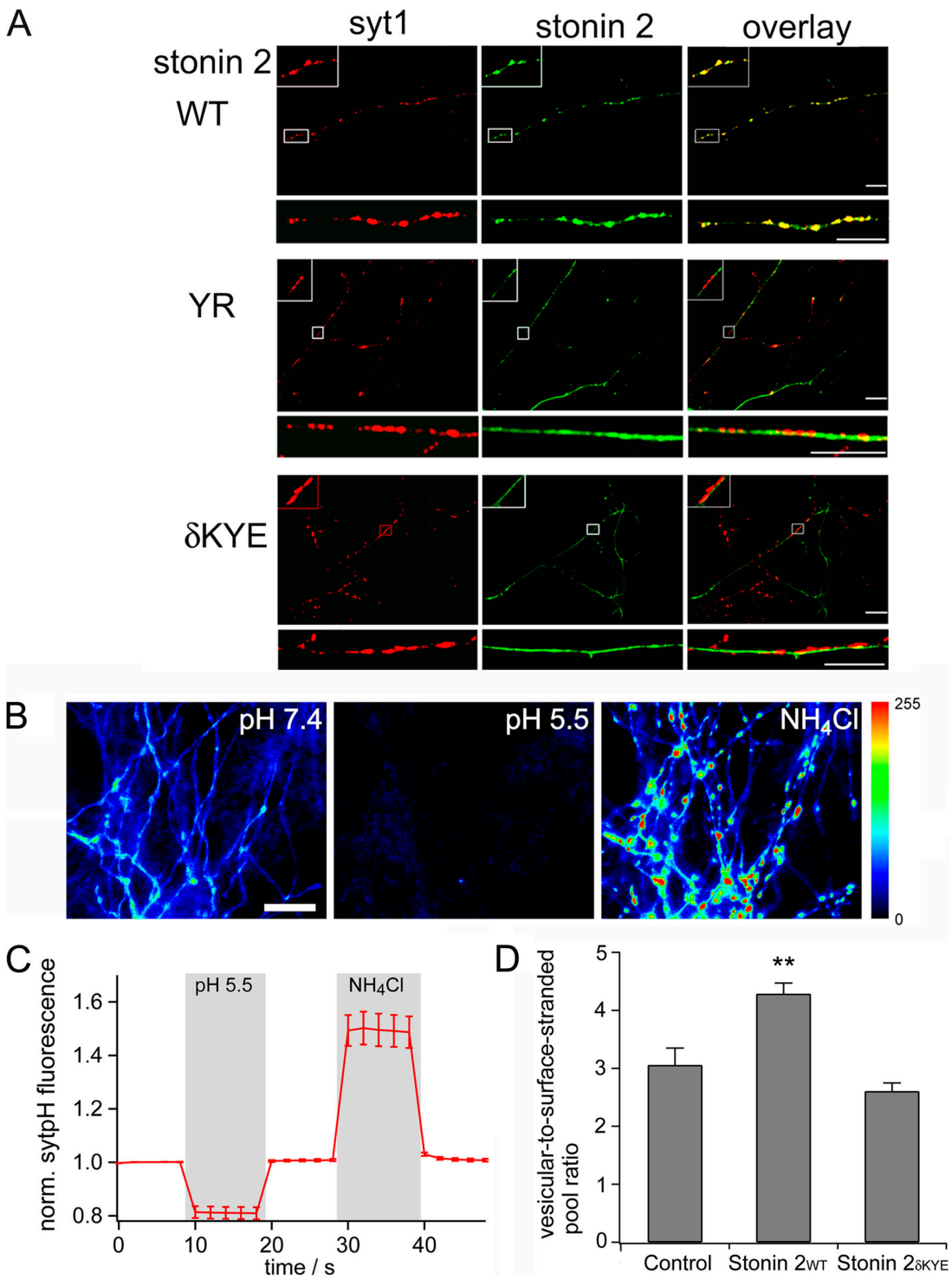

Figure 6. **The stonin 2 KYE site is required for synaptic localization of stonin 2 and facilitates targeting of synaptotagmin 1 to recycling vesicles in primary neurons.** (A) Primary hippocampal neurons at DIV9 were transfected with HA–stonin 2^{WT}, –stonin 2^{YR}, or –stonin $2^{\delta KYE}$, respectively. Monoclonal antibodies against synaptotagmin 1 are used to decorate presynaptic sites (red). Low-power views (top) exemplify the overall distribution of HA-tagged stonin 2 or mutants (green; insets, threefold magnified images of boxed area). High-power views (bottom) represent the localization of HA–stonin 2 or mutants in selected neurites. Bars, 10 μm. (B–D) Stonin 2^{WT} but not stonin $2^{\delta KYE}$ mutant enhances targeting of sytpHluorin to recycling vesicles in primary hippocampal neurons. (B) To assess the surface and vesicular pools of sytpHluorin, the relative fluorescence (F) values were measure after acid quenching and ammonium dequenching. Bar, 10 μm. (C) Quantitative analysis of $n = 7$ experiments, each comprising >50 boutons as in B. Mean time course of sytpHluorin at synaptic boutons normalized to initial F values is shown. (D) Ratios of vesicular/surface stranded pools of sytpHluorin ($n = 7$ experiments; error bars represent SEM; control, 3.05 ± 0.3; stonin 2^{WT}, 4.28 ± 0.19; stonin $2^{\delta KYE}$, 2.6 ± 0.15; **, $P < 0.01$). Expression of WT stonin 2 results in a significant increase in the vesicular/surface pool ratio, whereas stonin $2^{\delta KYE}$ has lost this ability.

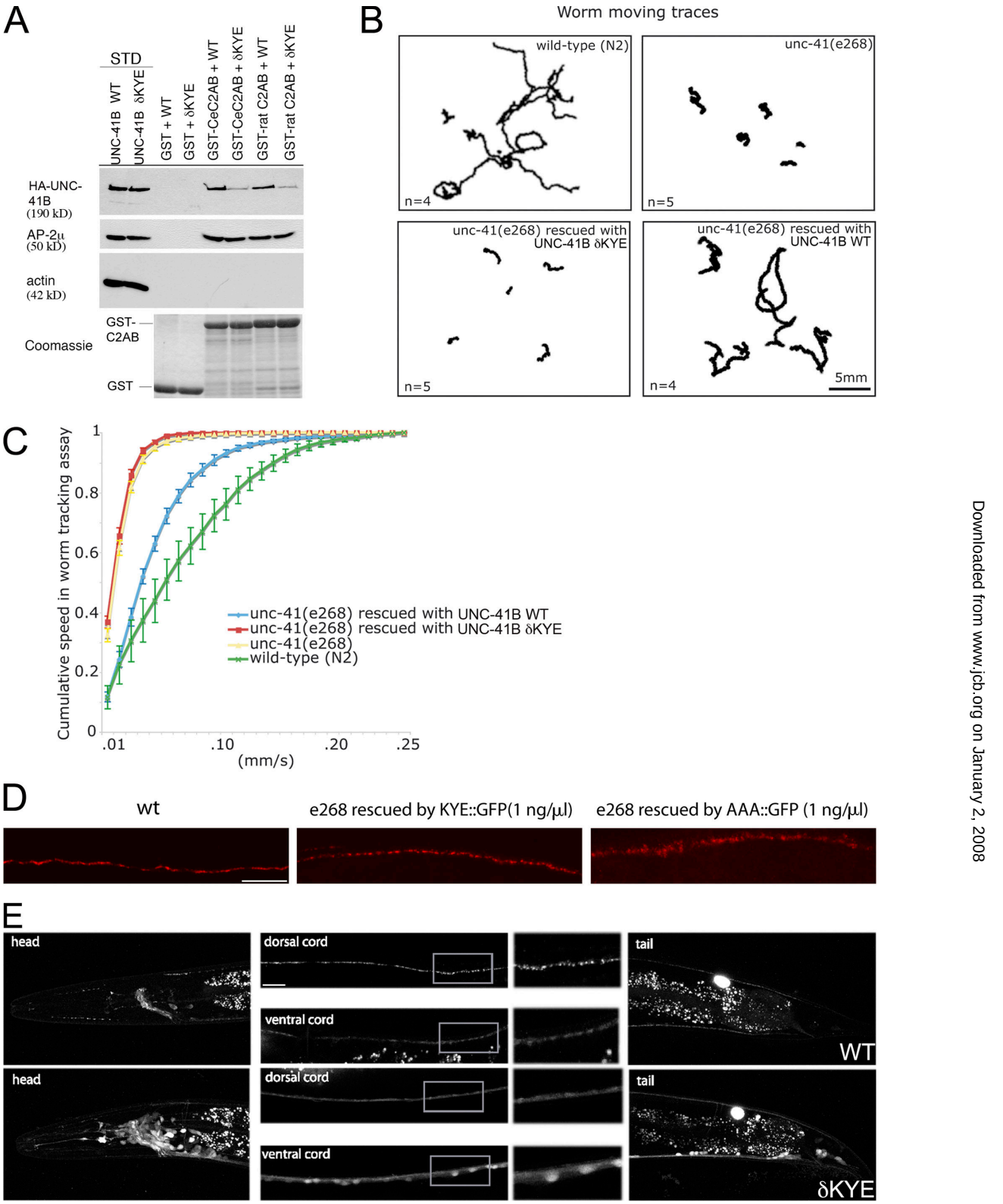

Figure 7. **The KYE site is required for UNC-41 function in locomotory behavior in *C. elegans*.** (A) Mutation of the KYE site within *C. elegans* UNC-41B abolishes its ability to bind to synaptotagmin 1. GST or GST fused to the C2 domains of rat or *C. elegans* (Ce) synaptotagmin 1 immobilized on 30-μg protein beads were incubated with cell extracts derived from Cos7 cells transfected with HA–UNC-41B or HA–UNC-41B δKYE. Bound proteins were detected by immunoblotting for HA–UNC-41B, actin, and AP-2μ. 4% of the input was loaded as standard. (B and C) Worm tracking assay for unc-41 mutant (*unc-41*) and rescued animals. (B) Representative worm moving traces over 10 min. The number of worms on each plate is indicated. (C) The mean speed for each 2 s was used and the percentage of the speed below a certain threshold was plotted for each genotype. Data are given as mean ± SEM. (D) Confocal images of immobilized worms expressing endogenous UNC-41 or plasmid-borne UNC-41B WT or the δKYE mutant analyzed by indirect immunofluorescence microscopy using UNC-41–specific antibodies. Bar, 10 μm. (E) Confocal images of immobilized worms expressing GFP–UNC-41B WT or the δKYE mutant. A magnified view of the boxed area from the dorsal cord is shown to the right of the image. Bar, 10 μm.

Third, direct binding, as well as coimmunoprecipitation experiments, reveals that conserved basic residues within C2A form the main interaction site for stonin 2. In contrast, AP-2 predominantly associates with the C2B domain, which is consistent with earlier data (Chapman et al., 1998; Haucke et al., 2000). We hypothesize that the identified basic patch within the C2A domain is part of an endocytosis signal. However, synaptotagmin 1 mutants displaying reduced affinity for stonin 2 (Fig. 2 D) appeared to retain the ability to undergo stonin 2–dependent internalization (not depicted), suggesting that additional determinants and/or cooperative effects are likely to be involved. It is worthwhile to note that both C2 domains contain additional positively charged surface-exposed side chains that could well serve as additional interaction sites for stonin 2.

Site-directed mutagenesis paired with structure-based homology modeling has allowed us to unravel the cognate recognition site for synaptotagmin 1 within the μHD of stonin 2. Mutational analysis reveals the functional importance of a β strand, including residues K783–E785, that is evolutionarily conserved between different members of the stonin/stoned B family of adaptors from nematodes to mammals (Fig. 3 A). We propose that the function of stonin 2 as a synaptotagmin-specific endocytic sorting adaptor dedicated to SV recycling is based on the ability of residues outlined by the KYE site to interact with patches of basic side chains within the synaptotagmin C2 domains. This proposal is based on the observations that stonin $2^{\delta KYE}$ is unable to interact with synaptotagmin directly in vitro or in living cells, to facilitate synaptotagmin 1 endocytosis in fibroblasts, to become enriched at presynaptic sites in primary neurons, or to target synaptotagmin 1 to the recycling vesicle pool at synapses. As with all mutant proteins, a valid concern is that the mutations may affect protein structure and/or stability. We feel that this is unlikely for several reasons. When expressed in fibroblasts or primary neurons, stonin $2^{\delta KYE}$ appeared to be expressed at levels comparable to those of its WT counterpart. Moreover, it retained its ability to associate with AP-2 in vitro and in living cells or to become targeted to clathrin-coated pits in primary astrocytes (unpublished data). When probed for structural integrity by limited proteolysis using different proteases, two independent mutants of stonin 2 (δKYE and Y784R) gave rise to fragmentation patterns virtually identical to those seen for the WT. A possible, yet speculative model for the recognition of synaptotagmin 1–C2A by the μHD of stonin 2 based on our collective mapping data is shown in Fig. S5 (available at http://www.jcb.org/cgi/content/full/jcb.200708107/DC1). Considering the high degree of sequence conservation with regard to synaptotagmin 1–C2 domains and stonin/stoned B family members, we consider it likely that other stonins, such as stoned B in *D. melanogaster* and UNC-41 in *C. elegans*, use a similar mode of cargo recognition.

One of the remaining puzzles is the observation that synaptotagmin 1 displays binding affinity for the ubiquitous adaptor AP-2μ and, in this respect, joins a growing number of pre- and postsynaptic proteins that use similar modes of recognition by AP-2μ for regulated endocytosis, including AMPA-type glutamate (Kastning et al., 2007) and $GABA_A$ receptors (Kittler et al., 2005). However, in vivo synaptotagmin endocytosis is strongly facilitated by its direct association with stonin 2 (Figs. 5, 6, and 7). This phenotype is even more pronounced in *D. melanogaster*, where stonin 2/stoned B is encoded by an essential gene (Fergestad and Broadie, 2001; Stimson et al., 2001). One possibility to explain the pivotal roles of stoned proteins could be the need for sorting during SV cycling. SV recycling requires constitutive cargo to be excluded from the forming vesicle and, thus, might benefit from the presence of a specific stonin family sorting adaptor. The presence of stonin 2 allows concentration of SV proteins, including synaptotagmin 1 and its partners, independently of the requirements of AP-2 for recognition of constitutive cargo (i.e., activation by kinases such as adaptor-associated kinase 1 and cyclin G–associated kinase), such as transferrin or EGF receptors. In addition, the use of C2A as an interaction interface for stonin 2 may alleviate constraints on SV cargo recognition imposed by the multiplicity of binding partners targeting the C2B domain of synaptotagmin 1. Multiple mechanisms of regulation of SV endocytosis by synaptotagmin 1 have recently been observed in *D. melanogaster* (Poskanzer et al., 2006). Mechanistically, the action of stonin 2 and its orthologues stoned B (*D. melanogaster*) and UNC-41B (*C. elegans*) may therefore resemble that of other CLASPs, including β-arrestins (Traub, 2005) or dishevelled-2 (Yu et al., 2007), in targeting cargo to subsets of clathrin-coated vesicles (Puthenveedu and von Zastrow, 2006). In the case of the presynaptic compartment, a precise fine tuning of the endocytic process is required to maintain the exact composition of SV proteins and lipids (Takamori et al., 2006) and to ensure release competence. The present study could form a first basis for the mechanistic understanding of this process.

Materials and methods

Cell culture and transfections

HEK293 and NIE-115 cells were cultured in DME (Invitrogen) containing 4.5 g/liter glucose and NIE cells in DME containing 1 g/liter glucose, supplemented with 10% FCS, penicillin, and streptomycin. Culturing of primary hippocampal neurons has been previously described (Mueller et al., 2004). Cell lines as well as primary neurons were transfected using Lipofectamine 2000 (Invitrogen). Calcium phosphate transfection was used for sytpHluorin recycling assays. Doxycycline-regulable HEK293 cell lines were generated using the T-Rex system (HEK^{TR}-$stn2^{WT}$, HEK^{TR}-$stn2^{\delta KYE}$; Invitrogen). HEK293 cells stably expressing lumenally FLAG-tagged synaptotagmin 1 (HEK-syt1) have been previously described (Diril et al., 2006). For morphological experiments, cells were grown on Matrigel-coated glass coverslips.

Plasmids and DNA constructs

The following amino terminally HA-tagged human stonin 2 constructs were made by inserting PCR products into EcoRV–XbaI restriction sites in pcHA2: HA–stonin 2 (aa 421–898), HA–stonin 2 (aa 1–555), and HA–stonin $2^{\delta WWW}$ (W15A, W102A, and W232A). We generated plasmid construct, allowing for the expression of lumenally FLAG-tagged rat synaptotagmin 1 by introducing the cDNA into the BamHI–XhoI restriction sites into the pcFLAG vector. By application of PCR site-directed mutagenesis, we prepared several synaptotagmin 1 mutation constructs: ΔC2B (1–265), ΔC2A (Δ140–270), ΔC2AB (1–139), and $syt1^{mut}$ (K189–192E; K213E; K244E; and KR321,322EE, K324–327E). The following rat synaptotagmin 1 GST fusion constructs were generated using pGEX4T-1 (BamHI–XhoI): C2A (140–265), C2B (271–421), C2AB (140–421), $C2A^{mut1}$ (KK189, 190AA), $C2A^{mut2}$ (KK191, 192AA), $C2A^{mut3}$ (K189–192A), $C2A^{mut4}$ (K191H, K213E, and K244S), $C2A^{mut5}$ (K189–192A, K213E, and K244S), $C2B^{mut1}$ (KK326, 327AA), $C2B^{mut2}$ (K324–327A), and $C2B^{mut3}$ (KR321, 322AA; and K324–327A). Constructs allowing for the expression of HA-tagged human stonin 2 were generated as previously described (Walther et al., 2004; Diril et al. 2006). The following mutants were prepared by PCR

site-directed mutagenesis: HA-stonin $2^{\delta WWW}$ (W15A, W102A, and W232A), HA-stonin $2^{\delta WF\delta NPF}$ (WF15, 18AA; WF102, 105AA; WF232, 235AA; NPF313–315NAV; and NPF329–313NAV), HA-stonin $2^{\delta KYE}$ (KYE783–785AAA), HA-stonin $2^{\delta WF\delta NPF\delta KYE}$ (WF15, 18AA; WF102, 105AA; WF232, 235AA; NPF313–315NAV; NPF329–313NAV; and KYE783–785AAA), HA-stonin 2^{KA} (K783A), HA-stonin 2^{YA} (Y784A), HA-stonin 2^{EA} (E785A), and HA-stonin 2^{YR} (Y784A). *C. elegans* synaptotagmin 1 C2AB (worm base: F31E8.2a [WS]; aa 158–441) was cloned into pGEX4T-1.

The GFP–UNC-41B WT (pMG13) *C. elegans* expression plasmid consisted of the 2.5-kb *unc-41* promoter (from RM536), 0.85-kb GFP fragment (from fire lab vector 95.77), and 5.4-kb *unc-41b* cDNA plus 3′UTR (from RM 536) inserted into the EcoRI–SalI restriction sites of pGEM-3zf(+) using the following primers: 5′-AGGAGAATTCCTCCCGGCAATTCGTAATACGTC-3′; 5′-GGGTCCTGAAAATGTTCTATG-3′; 5′-ACATTCCCGGGATGGAACAAG-CAGAAAAAGCA-3′;5′-ACTTGTCGACCATGTGTCAGAGGTTTTCACCGTC-3′; 5′-AGATCCCGGGAGAACCTCCGCCTCCTTTGTATAGTTCATCCATGCC-ATG-3′; and 5′-ACCGCCCGGGATGAGTAAAGGAGAAGAACTTTTC-3′.

An analogous construct was made for expression of the GFP–UNC-41B δKYE mutant (pMG14, *UNC-41* KYE→AAA translational GFP).

Antibodies

Polyclonal anti–stonin 2 antiserum was generated as described previously (Walther et al., 2004). Monoclonal antibodies against the α subunit of AP-2 (clone AP6) and clathrin heavy chain (clone TD1) were a gift from P. De Camilli (Yale University, New Haven, CT). Mono- (clone M2) or polyclonal anti-FLAG, as well as anti–β-actin antibodies, were obtained from Sigma-Aldrich, monoclonal anti-HA antibodies were obtained from Babco, polyclonal anti-HA antibodies (Y11) were obtained from Santa Cruz Biotechnology, Inc., monoclonal antibodies directed against the His_6-tag were obtained from EMD, monoclonal anti-α, -β2, and -μ2 antibodies were obtained from BD Biosciences, and monoclonal anti–synaptotagmin 1 antibodies (clone 41.1) were obtained from Synaptic Systems GmbH. Fluorescent dye–conjugated secondary antibodies were obtained from Invitrogen and horseradish peroxidase–labeled secondary antibodies, as well as unlabeled goat anti–mouse and goat anti–rabbit antibodies were obtained from Dianova GmbH.

Protein expression and purification

GST–synaptotagmin 1 fusion proteins were expressed in *Escherichia coli* (ER2566) at 25°C for 3 h after induction with 0.5 mM IPTG. Bacterial pellets obtained from 1-liter cultures were resuspended in 100 ml PBS. Cells were lysed using lysozyme, 1% Triton X-100, benzonase (to remove possible nucleic acid contaminants), and sonification. The bacterial extract was cleared by centrifugation at 39,000 *g* for 15 min and GST fusion proteins were affinity purified using GST-bind resin (EMD).

Stonin 2 WT and δKYE mutant proteins were affinity purified from HEK^{TR}-$stn2^{WT}$ and HEK^{TR}-$stn2^{\delta KYE}$ cells using Ni-NTA Agarose (QIAGEN). Protein expression was induced by addition of 1 μg/ml doxycycline to the growth medium for at least 16 h before cells were lysed in homogenization buffer (20 mM Hepes, pH 7.4, 150 mM NaCl, 2 mM $MgCl_2$, 1 mM PMSF, and 0.1% mammalian protease inhibitor cocktail [Sigma-Aldrich]) using a ball-bearing cell cracker with a clearance of 12 μm. The cell extract was cleared by consecutive centrifugation at 20,000 *g* for 5 min and 180,000 *g* for 15 min. The supernatant was supplemented with 320 mM sucrose, 500 mM NaCl, 1% CHAPS, 1 mM DTT, 10 mM imidazole, and 1 mM PMSF before application on Ni-NTA Agarose for 2 h at 4°C on a rotating wheel. The beads were washed twice in washing buffer (20 mM Hepes, pH 7.4, 500/150 mM NaCl, 2 mM $MgCl_2$, 320 mM sucrose, 1% CHAPS, 1 mM DTT, and 10 mM imidazole) containing 500 mM NaCl and once with washing buffer containing 150 mM NaCl. Bound protein was eluted in washing buffer containing 150 mM NaCl and 120 mM imidazole.

Affinity chromatography, in vitro binding, and immunoprecipitation experiments

24–48 h after transfection, transiently transfected HEK293 cells were lysed in 20 mM Hepes, 100 mM KCl, 2 mM $MgCl_2$, 1% Triton X-100, 1 mM PMSF, 0.3% mammalian protease inhibitor cocktail for 10 min on ice. Cleared cell extracts were incubated with GST fusion proteins on a rotating wheel (1 mg of cell extract at 1 mg/ml) for 2 h at 4°C. After extensive washes, bound proteins were eluted with 80 μl of sample buffer. For immunoprecipitation experiments, transfected HEK293 cells were lysed in the buffer specified in the preceding paragraph. Monoclonal antibodies immobilized on protein A/G–Sepharose (Santa Cruz Biotechnology, Inc.) were incubated with 1 mg of cell extracts at 1 mg/ml for 4 h at 4°C under gentle agitation. Beads were washed extensively and eluted with 60 μl of sample buffer. Samples were analyzed by SDS-PAGE and immunoblotting. For in vitro binding experiments, 2–3 μg of immobilized GST–synaptotagmin 1 fusion proteins were incubated with 600 ng to 1 μg stonin 2–His_6 in 100 μl of binding buffer (20 mM Hepes, pH 7.4, 150 mM NaCl, 2 mM $MgCl_2$, 320 mM sucrose, 1% CHAPS, 1 mM DTT, and 10 mM imidazole) for 2 h at 4°C. After three washes in binding buffer, the beads were eluted in 50 μl of sample buffer. Samples were analyzed by SDS-PAGE and immunoblotting.

For some experiments, radioactively labeled ^{35}S-labeled stonin 2^{WT}, ^{35}S-labeled stonin 2^{YR}, or ^{35}S-labeled stonin $2^{\delta KYE}$, synthesized by the coupled TNT in vitro transcription/translation kit (Promega), was incubated with 2 μg GST–synaptotagmin 1 fusion proteins in 100 μl of binding buffer for 2 h at 4°C on a rotating wheel. After three washes in binding buffer, the beads were eluted in 50 μl SDS-PAGE sample buffer and the entire sample was applied to SDS PAGE. Bound ^{35}S-labeled stonin 2 was detected by autoradiography using the Cyclone PhosphoImager system (PerkinElmer).

Tryptic in gel digest and mass spectrometry

The SDS polyacrylamide gel, containing the proteins of interest, was stained using the freshly prepared colloidal Coomassie and destained according to the manufacturer's instructions (Roth). Gel bands were excised under clean conditions with new razor blades and cut into 1-mm^3 pieces. Gel fragments were transferred to a 500-μl reaction tube and incubated in a shaker in 20 μl of a 1:1 solution of acetonitrile/100 mM NH_4HCO_3 for 15 min. Samples were centrifuged for a short time and supernatant was exchanged for 100% acetonitrile and incubated for 5 min or until the gel pieces turned white. Acetonitrile was removed and gel pieces lyophilized for 10 min. For reduction of disulfide bridges, the lyophilized gel pieces were incubated in 20 μl of 100 mM DTT in 100 mM NH_4HCO_3 for 30 min at 56°C. After incubation, samples were centrifuged for a short time, supernatant was removed, and volume was measured. Gel fragments were again dehydrated twice by the addition of 20 μl of 100% acetonitrile. Cysteine residues were covalently modified by carbamidomethylation by addition of 20 μl of 55 mM iodacetamide in 100 mM NH_4HCO_3 and incubation for 20 min at room temperature in the dark. Supernatant was removed and exchanged for 100 mM NH_4HCO_3 and incubated for 15 min at room temperature. Gel pieces were incubated in 20 μl of 100% acetonitrile until they turned white and lyophilized for 10 min. 12.5 μg/ml trypsin in 25 mM NH_4HCO_3 was prepared and added to the lyophilized gel pieces (volume = 20 μl − volume of supernatant, measured after reduction in DTT + 3 μl). Samples were placed for 30 min on ice before incubation at 37°C overnight. Samples were centrifuged and again incubated at 37°C for 30 min before ∼3 μl of the supernatant was removed and subjected to mass spectrometric analyses.

Limited proteolysis

We performed limited proteolysis to assess the folding properties of stonin 2 mutants by digestion of stonin 2–His_6 purified from stable HEK cells or in vitro–transcribed/translated stonin 2. 0–20 μg/ml Trypsin and 0–80 ng/ml proteinase K were chosen for this purpose. Proteolysis reactions were performed in 20 mM Hepes, pH 7.4, 100 mM KCl, and 2 mM $MgCl_2$ for in vitro–translated stonin 2 and in 20 mM Hepes, pH 7.4, 150 mM NaCl, 2 mM $MgCl_2$, 320 mM sucrose, 1% CHAPS, 1 mM DTT, and 10 mM imidazole for purified stonin 2–His_6 for 10 min at 37°C. In vitro–translated digested protein was analyzed by SDS-PAGE and autoradiography and stonin 2–His_6 by immunoblotting for the His_6-tag.

Antibody internalization and membrane recruitment assays

For indirect immunofluorescence microscopy, HEK293 cells stably expressing FLAG–synaptotagmin 1 were cooled on ice and preincubated with polyclonal anti-FLAG antibodies in Optimem (Invitrogen) for 30 min at 10°C. After chase at 37°C for 20 min, cells were fixed in 4% PFA for 10 min. Surface-bound anti-FLAG antibodies were blocked with unlabeled goat anti–rabbit IgG (1:5) overnight at 4°C. Cells were permeabilized and processed for immunostaining using Alexa Fluor 488– or 594–labeled secondary antibodies. Synaptotagmin internalization in transfected HEK-syt1 cells was essentially done as previously described (Diril et al., 2006). Membrane recruitment experiments in NIE-115 cells were performed as in Diril et al. (2006).

Images were taken at room temperature by a charge-coupled device camera (AxioCam; Carl Zeiss, Inc.) mounted on an inverted microscope (Axiovert 200M; Carl Zeiss, Inc.) with an oil-immersion objective (63× 1.4 NA; Carl Zeiss, Inc.) illuminated and controlled by the Stallion Ratio Imaging system (Intelligent Imaging Innovations, Inc.). Imaging data were digitized, analyzed, and processed by nearest neighbor deconvolution with Slidebook 4.0.10 software (Intelligent Imaging Innovations, Inc.).

Slidebook 4.0.10 was used for quantifications based on data obtained from at least three independent experiments. Using equal exposure times, at least three low-magnification images were acquired from each experiment, yielding a minimum of nine datasets (each containing 5–20 transfected cells). The Mask function was applied on the fluorescence channel representing stonin 2 (stonin 2 mask). Fluorescence values representing internalized synaptotagmin 1 within the stonin 2 mask were calculated, and mean internalized synaptotagmin 1 fluorescence values (±SEM) per cell were estimated and plotted in a histogram. Background fluorescence was subtracted.

SytpHluorin recycling assays in living neurons

Published procedures were used to assay sytpHluorin recycling in neurons (Diril et al., 2006). In brief, hippocampal neurons from 1–3-d-old Wistar rats were transfected by calciumphosphate DNA coprecipitation and used after 11–14 d in vitro. Synaptic boutons were stimulated by electric field stimulation (platinum electrodes, 10-mm spacing, 200 pulses of 50mA and alternating polarity, 10 μM CNQX, and 50 μM AP-5 to prevent recurrent action potentials) at room temperature. Fast solution exchanges were achieved by a piezo-controlled stepper device (SF77B; Warner Instruments). Images were taken by a cooled slow-scan charge-coupled device camera (PCO; SensiCam-QE) mounted on an inverted microscope (Axiovert S100TV; Carl Zeiss, Inc.) with a water-immersion objective(63×1.2 NA; Carl Zeiss, Inc.) Imaging data were digitized and preanalyzed with Till Vision Software (Till Photonics) by using regions of interest to delimit puncta. For further analysis, the data were collected, normalized, and averaged using self-written macros in Igor Pro (Wavemetrics).

***C. elegans* strains, microinjection, and confocal imaging**

The following strains were used for rescue experiments: WT *C. elegans* (Bristol N2); CB268: *unc-41(e268)*; EG4499: *unc-41(e268); oxEx920[Punc-41A::unc-41B(unc-41B WT cDNA), Pcc::GFP]*; and EG4501: *unc-41(e268); oxEx922[Punc-41A::unc-41B(unc-41B KYE→AAA cDNA), Pcc::GFP]*. Strains used for confocal imaging were: EG4741: *oxEx1050[Punc-41A::GFP::unc-41B(cDNA WT), Pcc::GFP]*; EG4746: *oxEx1055[Punc-41A::GFP::unc-41B(cDNA KYE→AAA mutant), Pcc::GFP]*; EG4751: *unc-41(e268), oxEx1059[Punc-41A::GFP::unc-41B(cDNA WT), Pcc::GFP]*; and EG4753: *unc-41(e268), oxEx1061[Punc-41A::GFP::unc-41B(cDNA KYE→AAA mutant), Pcc::GFP]*; EG4774: *snt-1(md290), oxEx1071[Punc-41A::GFP::unc-41B(cDNA WT), Pcc::GFP]*.

For rescue experiments, 50 ng/μl *Punc-122::GFP* used as an injection marker was mixed with 1 kb DNA ladder (Fermentas) as carrier DNA to give a final DNA concentration of 100 ng/μl. RM#536p (*Punc-41A::unc-41B(cDNA)*), WT, or KYE→AAA mutant constructs or analogous GFP fusion proteins (pMG13/14: *Punc-41A::gfp:: unc-41B*) were injected at 1 ng/ml into *unc-41(e268)* mutant or WT animals.

Worms were immobilized with 2% phenoxyl propanol, and GFP fluorescence was imaged at room temperature on a confocal laser-scanning microscope (LSM5; Pascal) using an oil-immersion objective (plan-Neofluar 40× 1.3 NA; Carl Zeiss, Inc.) and analyzed by confocal software (Carl Zeiss, Inc.).

Worm-tracking assay

1% unseeded 50-mm agar plates containing 0.004% Bromphenol blue were prepared. Right before the assay, 200 ml 2% OP50 *E. coli* were spread onto the assay plates to analyze worm feeding behavior. Four to five worms were put on a single plate. Worm positions were recorded every 2 s for 10 min. Images were analyzed by worm tracker 06 (an ImageJ plug-in developed by J. White, University of Utah, Salt Lake City, UT). 300 mean speed values were collected for each worm. 6–10 worms were analyzed per genotype.

Molecular modeling and multiple sequence alignments

Multiple protein sequence alignments were performed using the ClustalW program (available at http://www.ebi.ac.uk/clustalw/). The x-ray structure of μ2 was used as a structural template for the model of stonin 2–μHD (G563-E875; 1GW5: chain M, G165-C435). Additional fragments with sequence homology to other known Protein Database structures (1BWU and 2FEA) were used to complete the model for residues 622–638 and 736–772 of stonin 2 for which corresponding loop regions in μ2 were not resolved or no homologous sequence was available in the μ2 template. The x-ray structure of synaptotagmin 1–C2A (1BYN: E140-K267) was used to create the interaction model shown in Fig. S5. Interaction models considering complementary shape, electrostatic potentials, and data from mutational analysis were generated by manual docking using the biopolymer module of SYBYL7.2 and minimized with an AMBER 7.0 force field within SYBYL (TRIPOS, Inc.).

Online supplemental material

Fig. S1 shows association of stonin 2 with synaptotagmin 1. Fig. S2 shows that stonin 2 directly binds to synaptotagmin 1 in vitro. Fig. S3 shows that the interaction between stonin 2 and synaptotagmin 1 depends on residues within the carboxy-terminal μHD of stonin 2. Fig. S4 shows that limited proteolytic digests of stonin 2 WT, δKYE, and YR mutants indicate structural integrity of the mutated proteins. Fig. S5 shows a hypothetical model of the interaction between stonin 2 (gray) and the C2A domain of synaptotagmin 1 (yellow) via two parallel β strands. Online supplemental material is available at http://www.jcb.org/cgi/content/full/jcb.200708017/DC1.

This work was supported by grants from the Deutsche Forschungsgemeinschaft (SFB449, TP A11, and HA2686/1-1, 1-2 to V. Haucke; and SFB523 and TP B10 to J. Klingauf), the German Federal Ministry of Science (BioDISC-2/RENTRAFF), and the Human Frontier Science Program (to J. Klingauf). N. Jung received initial support from the Lichtenberg Foundation and was a student of the International PhD Program in Molecular Biology at the University of Göttingen. M. Wienisch was a student of the International PhD Programin Neuroscience at the University of Göttingen and received support from the Boehringer Ingelheim Fonds. E. Jorgensen is an Investigator of the Howard Hughes Medical Institute, and this work was supported by a grant from the National Institutes of Health (NS034307).

Submitted: 15 August 2007
Accepted: 25 November 2007

References

Bai, J., W.C. Tucker, and E.R. Chapman. 2004. PIP2 increases the speed of response of synaptotagmin and steers its membrane-penetration activity toward the plasma membrane. *Nat. Struct. Mol. Biol.* 11:36–44.

Bennett, M.K., N. Calakos, T. Kreiner, and R.H. Scheller. 1992. Synaptic vesicle membrane proteins interact to form a multimeric complex. *J. Cell Biol.* 116:761–775.

Bonifacino, J.S., and L.M. Traub. 2003. Signals for sorting of transmembrane proteins to endosomes and lysosomes. *Annu. Rev. Biochem.* 72:395–447.

Brodin, L., P. Low, and O. Shupliakov. 2000. Sequential steps in clathrin-mediated synaptic vesicle endocytosis. *Curr. Opin. Neurobiol.* 10:312–320.

Chapman, E.R., R.C. Desai, A.F. Davis, and C.K. Tornehl. 1998. Delineation of the oligomerization, AP-2 binding, and synprint binding region of the C2B domain of synaptotagmin. *J. Biol. Chem.* 273:32966–32972.

Collins, B.M., A.J. McCoy, H.M. Kent, P.R. Evans, and D.J. Owen. 2002. Molecular architecture and functional model of the endocytic AP2 complex. *Cell*. 109:523–535.

DiAntonio, A., K.D. Parfitt, and T.L. Schwarz. 1993. Synaptic transmission persists in synaptotagmin mutants of *Drosophila*. *Cell*. 73:1281–1290.

Diril, M.K., M. Wienisch, N. Jung, J. Klingauf, and V. Haucke. 2006. Stonin 2 is an AP-2-dependent endocytic sorting adaptor for synaptotagmin internalization and recycling. *Dev. Cell*. 10:233–244.

Edeling, M.A., S.K. Mishra, P.A. Keyel, A.L. Steinhauser, B.M. Collins, R. Roth, J.E. Heuser, D.J. Owen, and L.M. Traub. 2006. Molecular switches involving the AP-2 beta2 appendage regulate endocytic cargo selection and clathrin coat assembly. *Dev. Cell*. 10:329–342.

Fergestad, T., and K. Broadie. 2001. Interaction of stoned and synaptotagmin in synaptic vesicle endocytosis. *J. Neurosci.* 21:1218–1227.

Galli, T., and V. Haucke. 2004. Cycling of synaptic vesicles: how far? How fast! *Sci. STKE*. 2004:re19.

Granseth, B., B. Odermatt, S.J. Royle, and L. Lagnado. 2006. Clathrin-mediated endocytosis is the dominant mechanism of vesicle retrieval at hippocampal synapses. *Neuron*. 51:773–786.

Grass, I., S. Thiel, S. Honing, and V. Haucke. 2004. Recognition of a basic AP-2 binding motif within the C2B domain of synaptotagmin is dependent on multimerization. *J. Biol. Chem.* 279:54872–54880.

Haucke, V., M.R. Wenk, E.R. Chapman, K. Farsad, and P. De Camilli. 2000. Dual interaction of synaptotagmin with mu2- and alpha-adaptin facilitates clathrin-coated pit nucleation. *EMBO J.* 19:6011–6019.

Jarousse, N., and R.B. Kelly. 2001. The AP2 binding site of synaptotagmin 1 is not an internalization signal but a regulator of endocytosis. *J. Cell Biol.* 154:857–866.

Jia, J.Y., S. Lamer, M. Schumann, M.R. Schmidt, E. Krause, and V. Haucke. 2006. Quantitative proteomics analysis of detergent-resistant membranes from chemical synapses: evidence for cholesterol as spatial organizer of synaptic vesicle cycling. *Mol. Cell. Proteomics*. 5:2060–2071.

Jorgensen, E.M., E. Hartwieg, K. Schuske, M.L. Nonet, Y. Jin, and H.R. Horvitz. 1995. Defective recycling of synaptic vesicles in synaptotagmin mutants of *Caenorhabditis elegans*. *Nature*. 378:196–199.

Kastning, K., V. Kukhtina, J.T. Kittler, G. Chen, A. Pechstein, S. Enders, S.H. Lee, M. Sheng, Z. Yan, and V. Haucke. 2007. Molecular determinants for the interaction between AMPA receptors and the clathrin adaptor complex AP-2. *Proc. Natl. Acad. Sci. USA*. 104:2991–2996.

Kittler, J.T., G. Chen, S. Honing, Y. Bogdanov, K. McAinsh, I.L. Arancibia-Carcamo, J.N. Jovanovic, M.N. Pangalos, V. Haucke, Z. Yan, and S.J. Moss. 2005. Phospho-dependent binding of the clathrin AP2 adaptor complex to GABAA receptors regulates the efficacy of inhibitory synaptic transmission. *Proc. Natl. Acad. Sci. USA*. 102:14871–14876.

Lefkowitz, R.J., and E.J. Whalen. 2004. beta-arrestins: traffic cops of cell signaling. *Curr. Opin. Cell Biol.* 16:162–168.

Littleton, J.T., J. Bai, B. Vyas, R. Desai, A.E. Baltus, M.B. Garment, S.D. Carlson, B. Ganetzky, and E.R. Chapman. 2001. synaptotagmin mutants reveal essential functions for the C2B domain in Ca2+-triggered fusion and recycling of synaptic vesicles in vivo. *J. Neurosci.* 21:1421–1433.

Llinas, R.R., M. Sugimori, K.A. Moran, J.E. Moreira, and M. Fukuda. 2004. Vesicular reuptake inhibition by a synaptotagmin I C2B domain antibody at the squid giant synapse. *Proc. Natl. Acad. Sci. USA*. 101:17855–17860.

Martina, J.A., C.J. Bonangelino, R.C. Aguilar, and J.S. Bonifacino. 2001. Stonin 2: an adaptor-like protein that interacts with components of the endocytic machinery. *J. Cell Biol.* 153:1111–1120.

Mishra, S.K., P.A. Keyel, M.J. Hawryluk, N.R. Agostinelli, S.C. Watkins, and L.M. Traub. 2002. Disabled-2 exhibits the properties of a cargo-selective endocytic clathrin adaptor. *EMBO J.* 21:4915–4926.

Mueller, V.J., M. Wienisch, R.B. Nehring, and J. Klingauf. 2004. Monitoring clathrin-mediated endocytosis during synaptic activity. *J. Neurosci.* 24:2004–2012.

Murthy, V.N., and P. De Camilli. 2003. Cell biology of the presynaptic terminal. *Annu. Rev. Neurosci.* 26:701–728.

Nicholson-Tomishima, K., and T.A. Ryan. 2004. Kinetic efficiency of endocytosis at mammalian CNS synapses requires synaptotagmin I. *Proc. Natl. Acad. Sci. USA*. 101:16648–16652.

Owen, D.J., and P.R. Evans. 1998. A structural explanation for the recognition of tyrosine-based endocytotic signals. *Science*. 282:1327–1332.

Poskanzer, K.E., K.W. Marek, S.T. Sweeney, and G.W. Davis. 2003. Synaptotagmin I is necessary for compensatory synaptic vesicle endocytosis in vivo. *Nature*. 426:559–563.

Poskanzer, K.E., R.D. Fetter, and G.W. Davis. 2006. Discrete residues in the c(2)b domain of synaptotagmin I independently specify endocytic rate and synaptic vesicle size. *Neuron*. 50:49–62.

Puthenveedu, M.A., and M. von Zastrow. 2006. Cargo regulates clathrin-coated pit dynamics. *Cell*. 127:113–124.

Santolini, E., C. Puri, A.E. Salcini, M.C. Gagliani, P.G. Pelicci, C. Tacchetti, and P.P. Di Fiore. 2000. Numb is an endocytic protein. *J. Cell Biol.* 151:1345–1352.

Stimson, D.T., P.S. Estes, S. Rao, K.S. Krishnan, L.E. Kelly, and M. Ramaswami. 2001. *Drosophila* stoned proteins regulate the rate and fidelity of synaptic vesicle internalization. *J. Neurosci.* 21:3034–3044.

Sudhof, T.C. 2004. The synaptic vesicle cycle. *Annu. Rev. Neurosci.* 27:509–547.

Takamori, S., M. Holt, K. Stenius, E.A. Lemke, M. Gronborg, D. Riedel, H. Urlaub, S. Schenck, B. Brugger, P. Ringler, et al. 2006. Molecular anatomy of a trafficking organelle. *Cell*. 127:831–846.

Traub, L.M. 2005. Common principles in clathrin-mediated sorting at the Golgi and the plasma membrane. *Biochim. Biophys. Acta*. 1744:415–437.

Voglmaier, S.M., K. Kam, H. Yang, D.L. Fortin, Z. Hua, R.A. Nicoll, and R.H. Edwards. 2006. Distinct endocytic pathways control the rate and extent of synaptic vesicle protein recycling. *Neuron*. 51:71–84.

Walther, K., M.K. Diril, N. Jung, and V. Haucke. 2004. Functional dissection of the interactions of stonin 2 with the adaptor complex AP-2 and synaptotagmin. *Proc. Natl. Acad. Sci. USA*. 101:964–969.

Wienisch, M., and J. Klingauf. 2006. Vesicular proteins exocytosed and subsequently retrieved by compensatory endocytosis are nonidentical. *Nat. Neurosci.* 9:1019–1027.

Willig, K.I., S.O. Rizzoli, V. Westphal, R. Jahn, and S.W. Hell. 2006. STED microscopy reveals that synaptotagmin remains clustered after synaptic vesicle exocytosis. *Nature*. 440:935–939.

Yu, A., J.F. Rual, K. Tamai, Y. Harada, M. Vidal, X. He, and T. Kirchhausen. 2007. Association of dishevelled with the clathrin ap-2 adaptor is required for frizzled endocytosis and planar cell polarity signaling. *Dev. Cell*. 12:129–141.

Zhang, J.Z., B.A. Davletov, T.C. Sudhof, and R.G. Anderson. 1994. Synaptotagmin I is a high affinity receptor for clathrin AP-2: implications for membrane recycling. *Cell*. 78:751–760.

Supplemental data

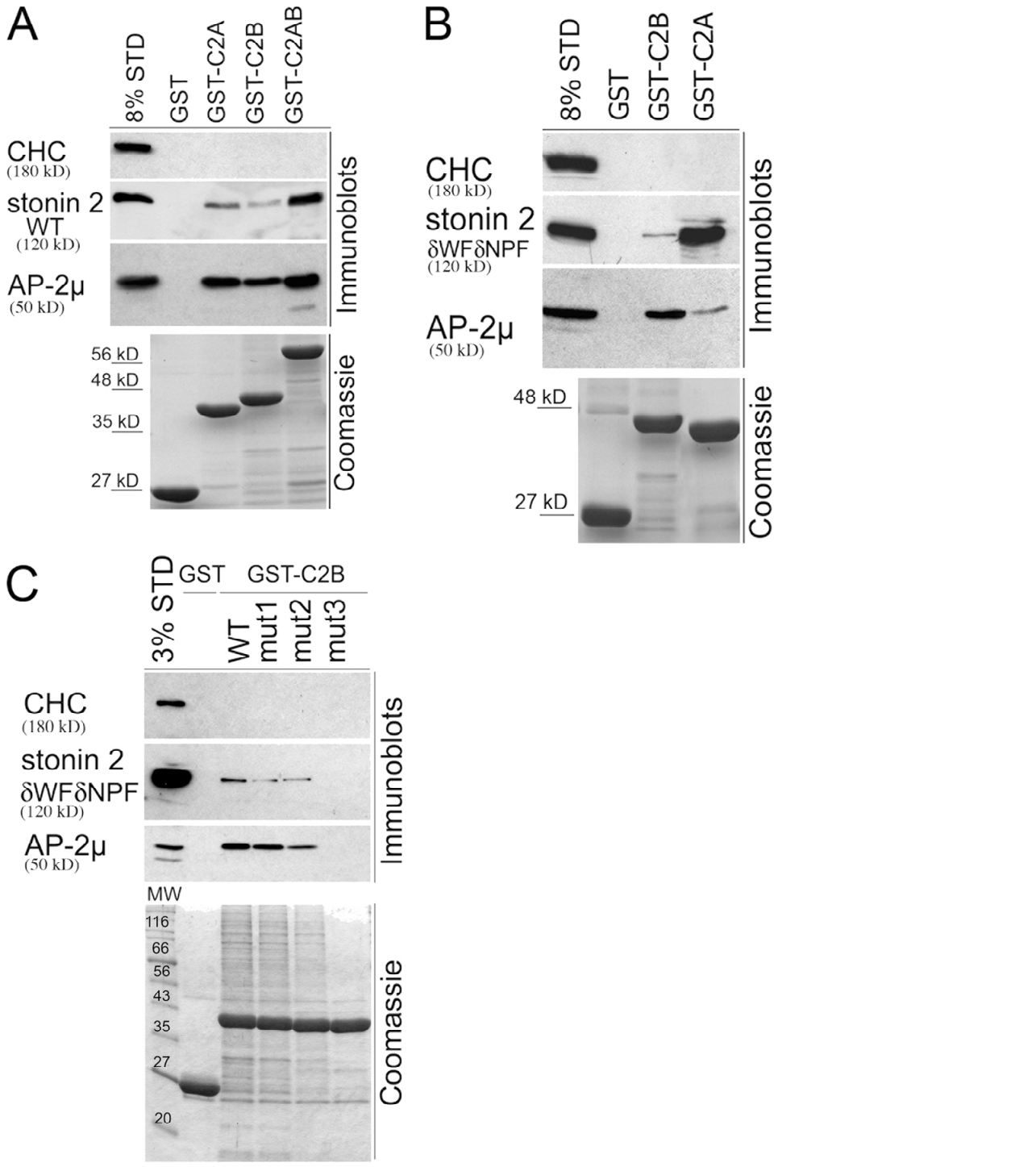

Figure S1. Association of stonin 2 with synaptotagmin 1. (A) 6 µg GST–synaptotagmin 1 cytoplasmic domain (C2A, C2B, or C2AB) fusion proteins (bottom) were analyzed in pulldown experiments for their ability to associate with HA–stonin 2WT from HEK293 cell lysates (Materials and methods). Samples were analyzed by immunoblotting (top) for HA–stonin 2, AP-2µ, or clathrin heavy chain (CHC). 8% standard (STD), 8% of the total input (cell extract). (B) Same as in A, but with an AP-2–binding–deficient HA–stonin 2δWFδNPF mutant. (C) GST-C2B wild-type or mutant proteins (Fig. 2 B) were analyzed in pulldown experiments for their ability to associate with HA–stonin 2δWFδNPF from HEK293 lysates. Samples were analyzed by immunoblotting for HA–stonin 2, AP-2β, and clathrin heavy chain. 3% of the input was loaded as standard.

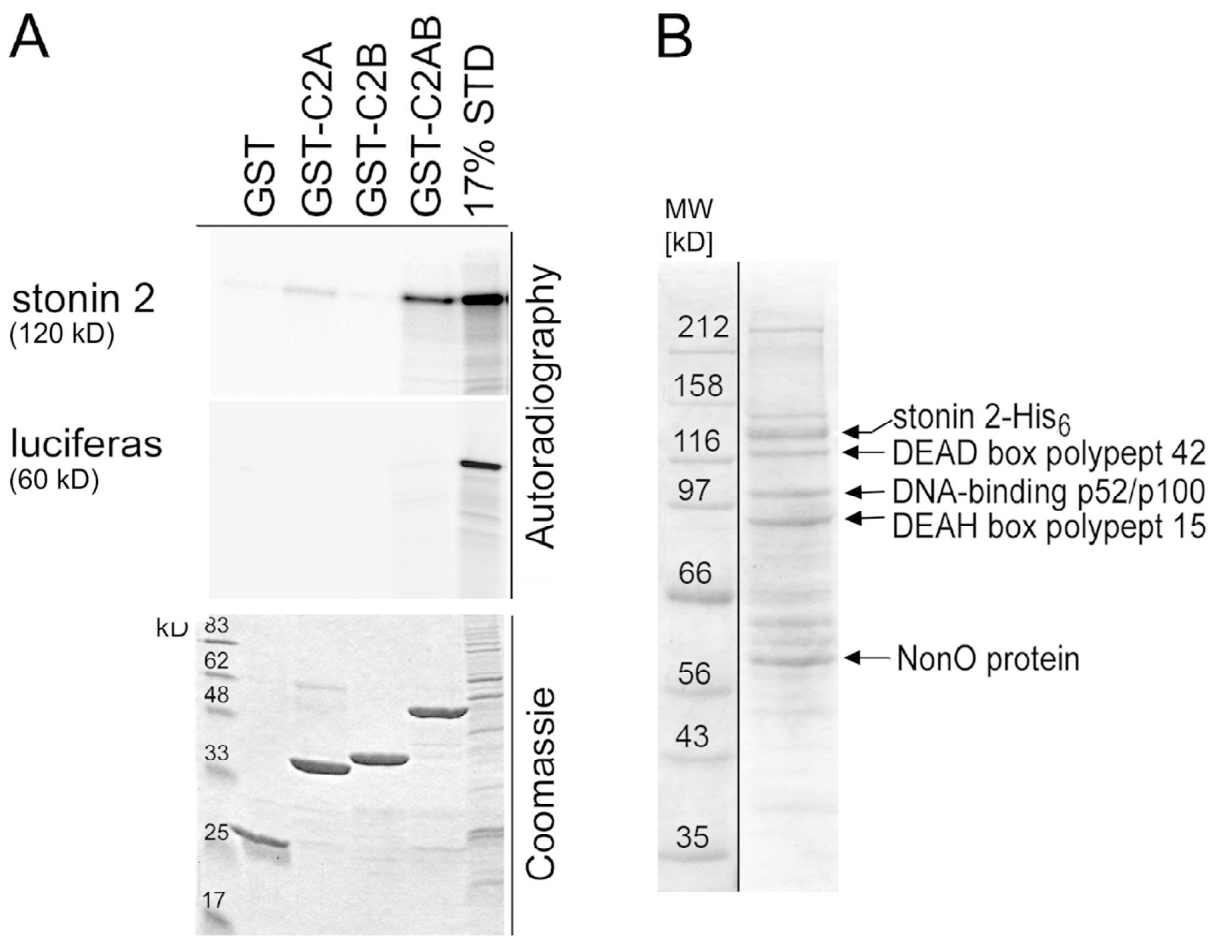

Figure S2. Stonin 2 directly binds to synaptotagmin 1 in vitro. (A) GST–synaptotagmin 1 fusion proteins immobilized on beads were incubated with 35S-labeled stonin 2 synthesized by coupled transcription/translation in vitro. 17% of 35S-labeled stonin 2 applied to the assay was loaded as standard. [35S]Luciferase served as negative control. (B) Stonin 2–His6 purified from stably transfected HEK293 cells. Contaminating bands were identified by mass spectrometry: DEAD box polypeptide 42 protein [Homo sapiens]/103 kD, Entry Q86XP3_HUMAN Score 209, E-value 4,8e-15, 26/45 matches; Splicing factor prolin/glutamin-rich (SFPQ protein)/76 kD, Synonym: DNA-binding p52/p100 complex, 100 kD subunit, Swiss-Prot entry SFPQ_HUMAN Score 86, E-value 0.00057, 10/15 matches; DEAH-box polypeptide 15/ 92 kD, Synonym: Putative premRNA-splicing factor ATP-dependent RNA helicase DHX15, Swiss-Prot entry DHX15_HUMAN, Score 88, E-value 0.00024, 14/33 matches; Similar to non-POU domain containing octamer-binding protein / 54 kD, Synonyms: NonO protein 54 kD nuclear RNA- and DNA-binding protein Swiss-Prot entry NONO_HUMAN Score 181, E-value 1.8e-13, 31/56 matches.

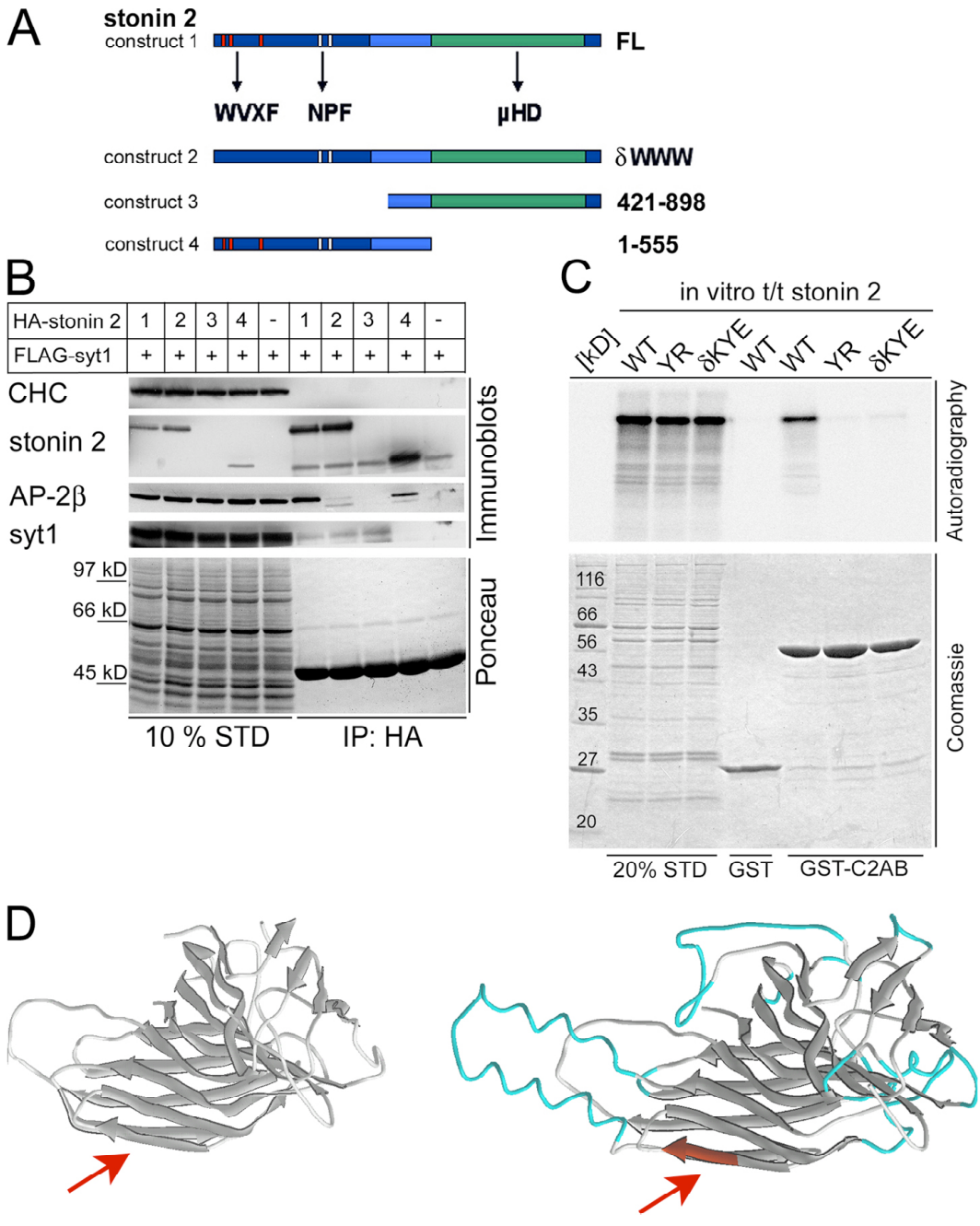

Figure S3. The interaction between stonin 2 and synaptotagmin 1 depends on residues within the carboxy-terminal μHD of stonin 2. (A) Stonin 2 constructs tested for synaptotagmin 1 interaction in B. (B) Coimmunoprecipitation experiments from fibroblast cell extracts. HEK293 cells stably transfected with FLAG-tagged synaptotagmin 1 (HEK-syt1) were transfected with HA-tagged stonin 2 constructs shown in A. Immunoprecipitation was performed using an antiserum directed against stonin 2. Coimmunoprecipitated proteins were detected by immunoblotting against FLAG-tag (syt1), β2-adaptin (AP-2β), HA-tag (stonin 2), and clathrin heavy chain as negative control. 10% of the input was loaded as standard. WVXF: AP-2–binding motif (δWWW: WVXF→AVXF). (C) Stonin 2 δKYE and YR mutations result in loss of interaction with synaptotagmin 1. 2 μg GST-C2AB fusion proteins were incubated with 35S-labeled stonin 2 synthesized by coupled transciption/translation in vitro. Bound stonin 2 was detected by autoradiography. 20% of the input material was loaded as standard. (D) Molecular homology model of the stonin 2 μHD (right) based on the crystal structure (1GW5_M) of AP-2μ as a main template (left). Modeled loops within stonin 2 that differ from the template are colored in cyan. The KYE site (783–785) within stonin 2 is depicted in red (arrow).

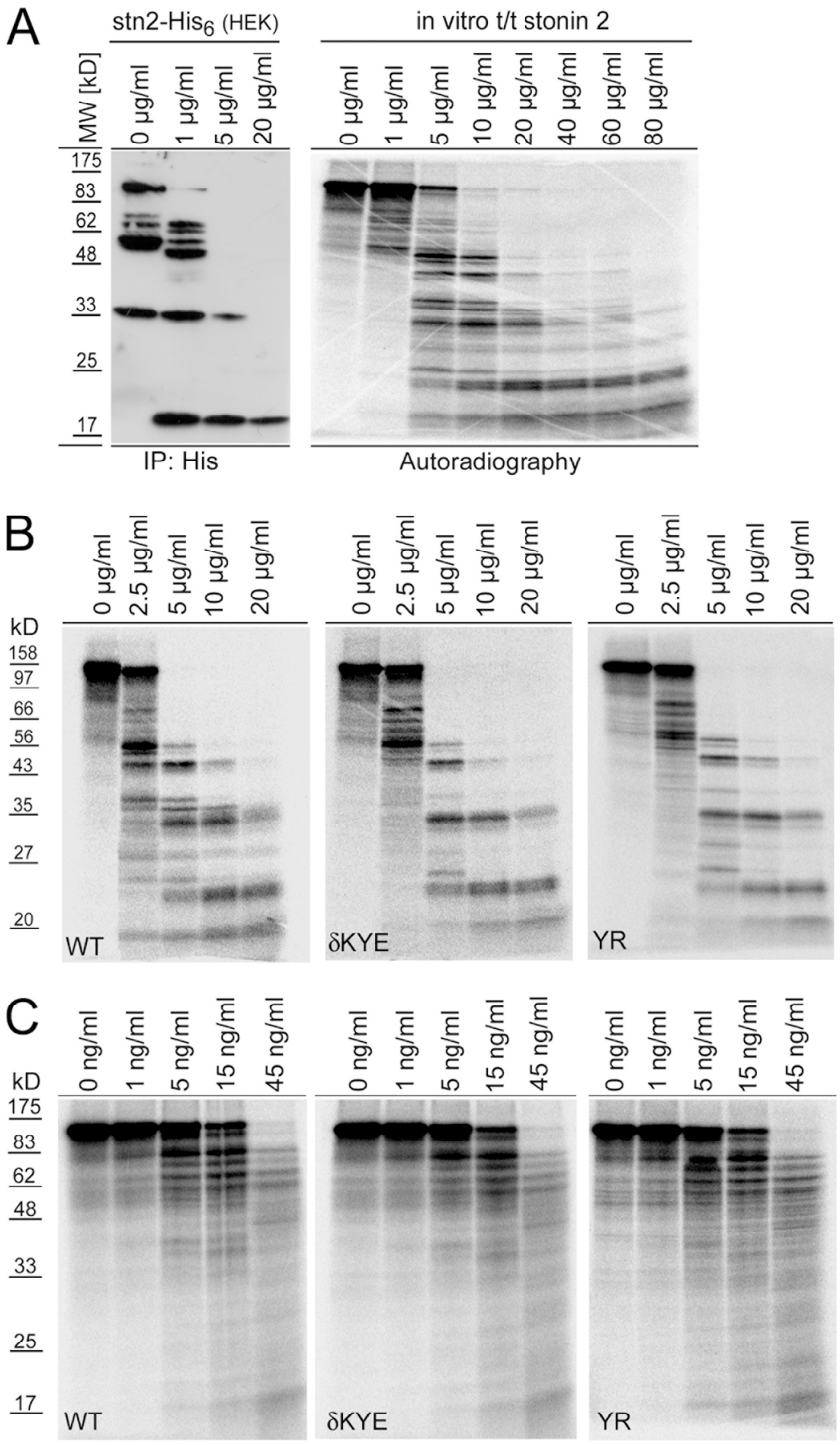

Figure S4. Limited proteolytic digests of stonin 2 wild-type, δKYE, and YR mutants indicate structural integrity of the mutated proteins. (A) Limited tryptic digests of carboxy-terminally His6-tagged stonin 2 purified from HEK293 cells or synthesized by coupled transcription/translation in vitro (in vitro t/t stonin 2). The digest was performed for 10 min at 37°C with the indicated concentrations of trypsin. (B) Limited tryptic digest of 35S-labeled stonin 2WT, 35S-labeled stonin 2δKYE, and 35S-labeled stonin 2YR result in similar digestion patterns. Proteins were digested as described in A. (C) Limited proteolysis experiment as described in B using proteinase K at the indicated concentrations.

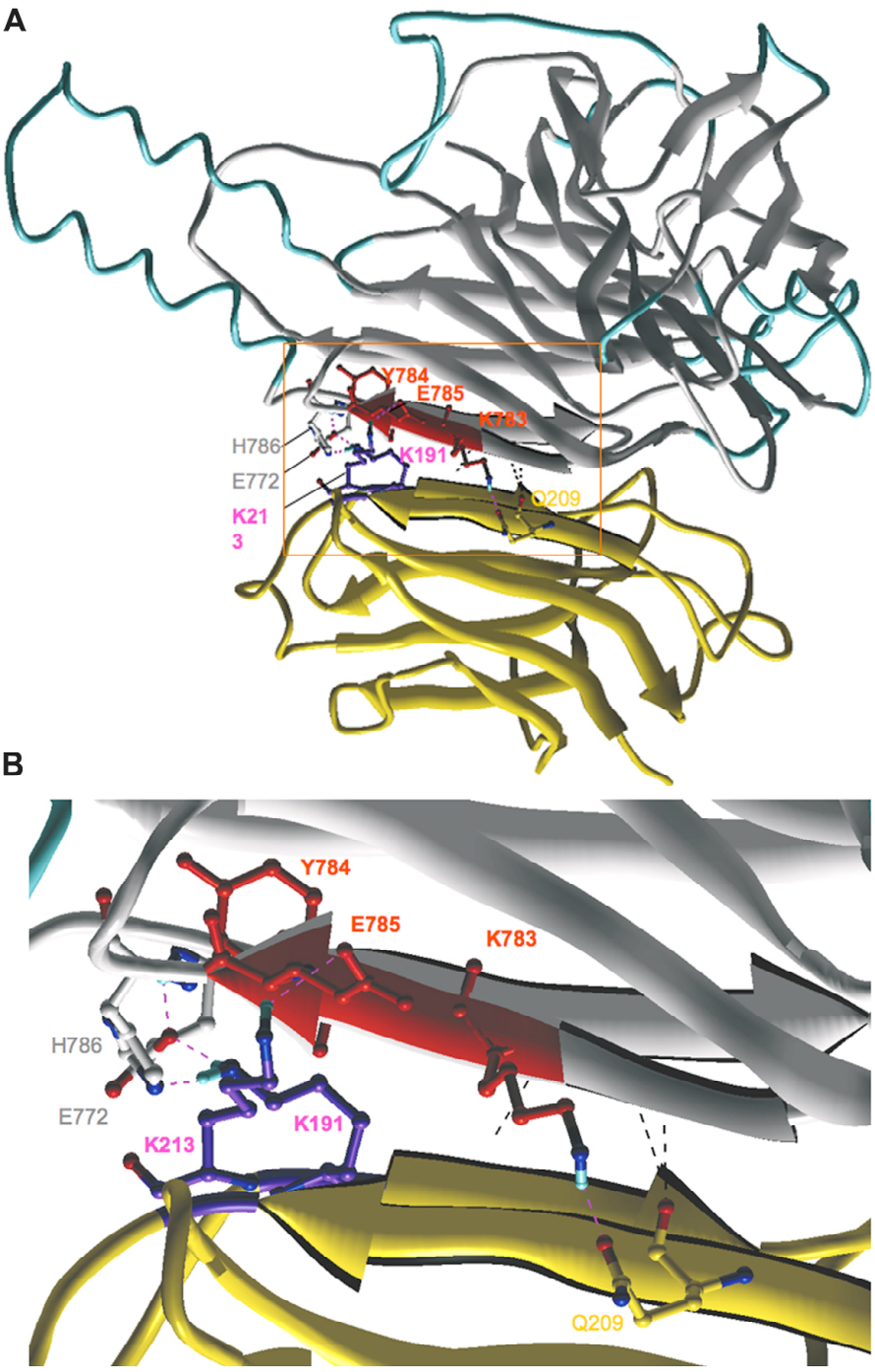

Figure S5. Hypothetical model of the interaction between stonin 2 (gray) and the C2A domain of synaptotagmin 1 (yellow) via two parallel β-strands. (A and B) B shows details of the possible interaction site marked by a rectangle in A. Purple dashed lines refer to putative hydrogen bonds between backbone atoms of β-strands and side chains within both protein domains. The KYE site (red arrow) within stonin 2 and basic side chains K191 and K213 (purple) within synaptotagmin 1–C2A are sensitive to mutation in protein–protein interaction assays.